J. Phys.: Condens. Matter **25** (2013) 035801 (28pp) doi:10.1088/0953-8984/25/3/035801

Positron annihilation on defects in silicon irradiated with 15 MeV protons

N Y Arutyunov[1,2], M Elsayed[1,3], R Krause-Rehberg[1], V V Emtsev[4], G A Oganesyan[4] and V V Kozlovski[5]

[1] Department of Physics, Martin Luther University Halle, D-06120 Halle, Germany
[2] Institute of Ionic-Plasma and Laser Technologies (Institute of Electronics), 700187 Tashkent, Uzbekistan
[3] Faculty of Science, Physics Department, Minia University, PO Box 61519 Minia, Egypt
[4] Ioffe Physico-Technical Institute, St Petersburg 194021, Russia
[5] St Petersburg State Polytechnical University, St Petersburg 195251, Russia

E-mail: n_arutyunov@yahoo.com and melabdalla@yahoo.co.uk

Received 14 July 2012, in final form 4 November 2012
Published 10 December 2012
Online at stacks.iop.org/JPhysCM/25/035801

Abstract

Microstructure and thermal stability of the radiation defects in n-FZ-Si ($[P] \approx 7 \times 10^{15}$ cm^{-3}) single crystals have been investigated. The radiation defects have been induced by irradiation with 15 MeV protons and studied by means of both the positron lifetime spectroscopy and low-temperature measurements of the Hall effect. At each step of the isochronal annealing over the temperature range ∼60–700 °C the positron lifetime has been measured for the temperature interval ∼30–300 K, and for samples-satellites the temperature dependences of the charge carriers and mobility have been determined over the range ∼4.2–300 K.

It is argued that as-grown impurity centers influence the average positron lifetime by forming shallow ($E_b \approx 0.013$ eV) positron states. The radiation-induced defects were also found to trap positrons into weakly bound ($E_b \leq 0.01$ eV) states. These positron states are observed at cryogenic temperatures during the isochronal annealing up to $T_{anneal.} = 340$ °C. The stages of annealing in the temperature intervals ∼60–180 °C and ∼180–260 °C reflect the disappearance of E-centers and divacancies, respectively.

Besides these defects the positrons were found to be localized at deep donor centers hidden in the process of annealing up to the temperature $T_{anneal.} \approx 300$ °C. The annealing of the deep donors occurs over the temperature range ∼300–650 °C. At these centers positrons are estimated to be bound with energies $E_b \approx 0.096$ and 0.021 eV within the temperature intervals ∼200–270 K and ∼166–66 K, respectively. The positron trapping coefficient from these defects increases from $\sim 1.1 \times 10^{16}$ to $\sim 6.5 \times 10^{17}$ s^{-1} over the temperature range ∼266–66 K, thus substantiating a cascade phonon-assisted positron trapping mechanism whose efficiency is described by $\approx T^{-3}$ law. It is argued that the value of activation energy of the isochronal annealing $E_a \approx 0.74$–0.59 eV is due to dissociation of the positron traps, which is accompanied by restoration of the electrical activity of the phosphorus atoms. The data suggest that the deep donors involve a phosphorus atom and at least two vacancies. Their energy levels are at least at $E > E_c - 0.24$ eV in the investigated material.

(Some figures may appear in colour only in the online journal)

1. Introduction

The production of the primary radiation defects in silicon doped with the phosphorus impurity results in, besides many other technologically important effects, a quasi-chemical reaction between vacancies and atoms of dopants whose products are the vacancy–impurity complexes. Among them E-centers are known to be relatively thermally unstable and

the electrical activity of the phosphorus dopant is restored by heat treatment at comparatively low temperatures, e.g., due to isochronal annealing from room temperature to 180–200 °C [1]. There is available exhaustive information on the energy levels of E-centers in the energy gap [2].

According to modern conceptions, the production rate of Frenkel pairs in silicon in the course of irradiation with fast electrons having energies of several MeV is much lower compared to protons and this difference is important from a practical point of view (see, e.g., review [3] and references therein). However, the information on the microstructure of the defects formed in silicon irradiated with 15 MeV protons is lacking.

For the first time we have undertaken a combined research of the microstructure of the radiation defects to be formed in n-FZ-Si single crystals in the course of irradiation with 15 MeV protons using two methods supplementing each other, namely, positron lifetime spectroscopy and low-temperature measurements of the Hall effect where the temperature dependences of the carrier concentration and their mobility have been reconstructed over the temperature range 4.2–300 K. Thus, the confidence in a reliable identification of the positron traps has either been supported or subjected to doubts in the course of analysis of the results obtained by both these methods. Also, in order to diminish any uncertainty related to an inhomogeneity in the distribution of as-grown defects and residual impurity centers in the single crystal, the samples used in both the experiments on positron annihilation and electro-physical measurements were cut from the same wafer.

The diffusion of positrons in the crystal is extremely sensitive to the presence of defects where the positron is capable of being partially localized (e.g., the shallow states of a comparatively large radius put limitations, at least, on both the positron mobility [4, 5] and the positron penetration into the ion cores of surrounding atoms [6]). The positron lifetime in such states is usually extremely close to one that is characteristic of the regular crystal lattice due to effective exchange between the localized and delocalized states owing to the positron–phonon interaction. However, when in the crystal vacancy-type defects are present the Coulomb interaction of the positron with the ion cores repels the positron, thus localizing it inside the area of the vacant site(s). The annihilation rate is known to be dictated by the electron density around the localized positron. As a rule, the electron density related to the vacancy (or vacancies in the many-vacancy defect) is lower than that in the bulk and this difference manifests itself in the data of measurements of the positron lifetime.

The doubling of doses used for irradiation of the samples resulted in an almost linear increase of the values of the average positron lifetime measured in the temperature interval ∼30–300 K (see below in more detail, section 2). Under such conditions the process of positron trapping is supposed to depend on the positron scattering in the bulk of silicon, where the centers formed by the residual impurities (such as, e.g., oxygen and carbon) create negative effective charges of the ion-covalent bonds. As a result, the positron wave packet is confined at these centers and positron localization (at least, the partial one) is observed [7]. In the first approximation, the states of such a kind are considered to be the shallow (Rydberg) states [8]; they may act as the states-precursors capable of localizing the positron before its trapping into a deeper state at the defects of a vacancy type [9].

We investigated the temperature dependency of the average positron lifetime in the bulk of an n-FZ-Si single crystal and found the shallow ($E_b \sim 0.01$ eV) states of positrons that might exist along with their localized states at the radiation defects.

The parameters of the positron lifetime are predetermined by the positron trapping coefficient as well as by the concentration of the positron-sensitive defects. The former is known to be a unique characteristic intimately related to both the configuration and chemical nature of the atoms involved into a microstructure of a positron trapping center. In order to estimate the positron trapping coefficient on the basis of the spectral data obtained by the positron annihilation methods, the knowledge of the concentration of the trapping centers is crucial. We measured the dependences of the carrier concentration over the temperature range ∼4.2–300 K in order to obtain numerical values of the concentration of the centers that were the positron traps; the samples-satellites to the ones used in the course of the positron lifetime measurements were under investigation.

There is experimental evidence indicating that the positron trapping by the radiation defects in the electron-irradiated silicon doped with phosphorus impurity depends on temperature and the character of this dependency is determined, in its turn, by the level of doping. In pure silicon the positron specific trapping rate (or the positron trapping coefficient) increases with the temperature decrease, reaching the values $\sim 10^{17}$–10^{18} s^{-1} at low temperature. In heavily doped float-zoned silicon Si($[P] = 10^{20}$ cm^{-3}) the radiation centers behave differently with respect to the trapping, manifesting themselves weakly in the data on measuring the temperature dependency of the average positron lifetime. It is argued that in pure silicon a negative single vacancy is the center responsible for the temperature dependency of the positron lifetime whereas in the heavily doped single crystal the negatively charged vacancy–phosphorus complex demonstrates independence of the positron trapping rate on the measurement temperature [10].

To make the reactions of the radiation-induced defects with the dopant much more pronounced, single crystal silicon having *a moderate* initial concentration of the phosphorus impurity has been investigated in this work. The isochronal annealing of the positron trapping centers in the proton-irradiated material was studied in detail. The two, rather low than moderate, doses were chosen in order to provide the trapping-limited regime for the positron movement in the irradiated material over the whole range of measurement temperatures.

It has been established that the positron-sensitive vacancy-type defects determine a complex behavior of the average positron lifetime in the course of the isochronal annealing. The latter reveals the centers demonstrating

properties of the deep donors; their annealing was found to be hidden in the process of healing of the other radiation defects at the earlier stages. These deep donors proved to be effective positron traps. They demonstrated complex behavior in the trapping and detrapping process in which the positron was established to be localized at both the shallow and relatively deep bound states. The body of evidence obtained suggests that the microstructure of the defects having properties of the deep donors involves vacancies and phosphorus atoms.

The paper is organized as follows. In section 2 experimental details are described. Section 3 begins with the analysis of experimental and calculated lifetimes obtained for initial samples at different temperatures. The positron lifetime parameters versus temperature under increasing proton irradiation doses are given in section 3.2. The positron trapping coefficients, the estimated positron trapping cross-sections at low doses of proton irradiation, and the binding energies of the positrons trapped at the radiation defects are presented in sections 3.3–3.6, respectively. Comparison of the calculated positron trapping coefficients with the experimental ones is given in section 3.7. Evidence of the phonon-assisted cascade positron trapping by the revealed defects possessing properties of deep donors is presented in section 3.8.

The data on isochronal annealing of the positron traps to be considered in their dependence on the annealing temperature and the temperature of measurements are presented in sections 3.9 and 3.10. The annealing of E-centers, divacancies, and oxygen-related (tentative) radiation defects is briefly described in sections 3.11–3.13. Thermo-dynamical parameters of annealing and the lifetime of positrons trapped at the revealed deep donors of radiation origin are considered in section 3.14. In section 3.15 the positron lifetime values obtained for deep donors are compared with the results of *ab initio* calculations available for vacancy clusters in silicon.

A discussion containing relevant data obtained earlier is given in section 4. A brief consideration of the results obtained from the point of view of relevant data on the as-grown oxygen-related centers in silicon is presented in section 4.1. Section 4.2 is concerned with the number of vacancies in the revealed positron traps, and the configuration of defects is considered, mainly, in the light of relevant data available for E-centers and divacancies. Shallow positron states that are thermally stable under the annealing of the irradiated material are briefly discussed in section 4.3. Positron trapping at the 'preparatory' stage of isochronal annealing and at the main stage are discussed in sections 4.4 and 4.5, respectively. Intimate relations between the microstructure of deep donors and the electrical activity of the phosphorus atoms is briefly touched upon in section 4.6. The conclusive remarks and a summary are in section 5.

In order to alleviate understanding and to avoid confusion, the temperature of annealing and the measurement temperature are given in generally accepted °C and K units, respectively. Also, for the reader's convenience, relevant parameters of the material are repeatedly shown in the figures and their captions when it is suitable or necessary.

2. Experimental details

2.1. Material and irradiation

The initial Si single crystal of n-type obtained by the floating-zone technique (n-FZ-Si) was moderately doped with phosphorus impurities $\sim$(6–8) $\times 10^{15}$ cm^{-3}. The samples used for the electro-physical measurements and for the positron annihilation studies were cut from the same wafer. The concentration of oxygen impurities did not exceed $\sim 5 \times 10^{16}$ cm^{-3}. The material was carbon lean; the concentration of carbon was a few units 10^{15} cm^{-3}.

The beam of 15 MeV protons penetrated through the samples having thickness $\leq$900 μm. At the exit of the sample the energy of protons was $E = 8$ MeV. So long as the rate of generation Q of the initial radiation defects is very roughly proportional to E^{-1} we have $\leq 2Q$ (15 MeV) at the surface of the exit of protons from the sample. The irradiation was carried out at room temperature; the results obtained for two doses, 4×10^{13} and 8×10^{13} cm^{-2}, are considered below. The stoppage effects may be neglected and the primary radiation defects have been produced quite homogeneously in the investigated samples since the projected range of the protons possessing energy 15 MeV is beyond $\sim 10^3$ μm.

2.2. Measurements of the Hall effect and electrical conductivity

The concentrations of the induced defects were determined from the temperature dependences of the concentrations of charge carriers and mobility measured over the range $\sim$4.2–300 K, for details of the procedure of analysis of these dependences, see, e.g. [11, 17, 18] and references therein. As an example, two typical dependences of the carrier concentration on the reciprocal temperature, $n(1/T)$, are shown in figure 1 for the initial material and the irradiated one.

2.2.1. Estimation of the concentration of the radiation-induced centers. Analysis of the temperature dependences $n(1/T)$ using the equations of the charge balance enabled us to evaluate separately both the total concentration of shallow donor centers and the concentration of compensating acceptors (for more details see, e.g. [11, 12] and references therein). The plateau region of the dependency shown in figure 1 goes down with an increasing dose of irradiation. The difference between the initial position of the plateau and the one to be observed after irradiation is used to determine the rate of carrier removal from the conduction band under proton irradiation (η_e), which in the present experiments proved to be equal to $\eta_e \approx 110$ cm^{-1} (silicon has been selected to obtain this numerical value, which is in a good agreement with the one published earlier [3, 11, 12, 17]). In order to determine what kind of the radiation defects causes a decrease of the electron concentration we have carried out an analysis of the $n(1/T)$ dependences on the basis of the corresponding electroneutrality equations for non-degenerate semiconductors (see, e.g., [17, 18] and references therein).

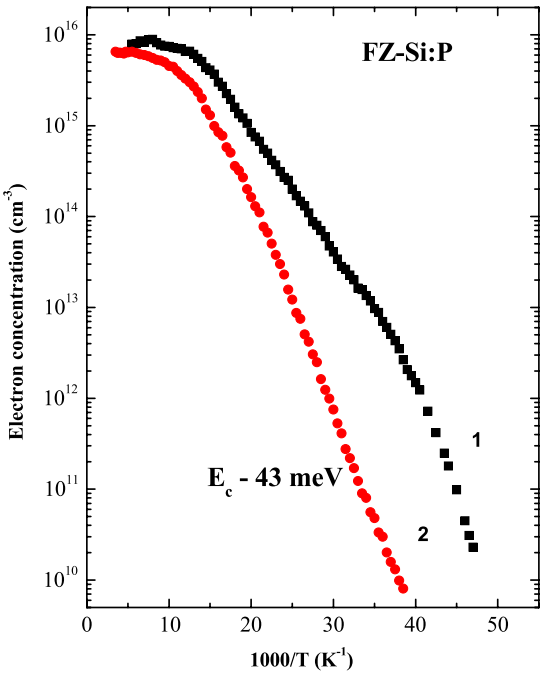

Figure 1. Carrier concentration versus reciprocal temperature in n-FZ-Si ($[P] \approx 7 \times 10^{15}$ cm^{-3}) before (1) and after (2) irradiation with 15 MeV protons, dose 3×10^{13} cm^{-2}. The ionization energy of shallow donors ∼47 meV (phosphorus) is shown; these dependences have been discussed in more detail previously [12].

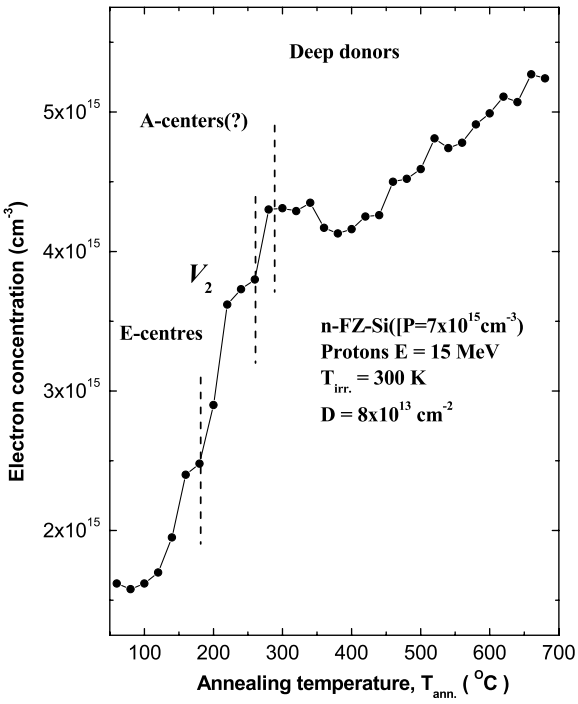

Figure 2. The carrier concentration values versus temperature of isochronal annealing ($h_T = 20\,^\circ$C/$t = 10$ min) reconstructed from the temperature dependences of the concentration of free charge carriers obtained over the range of ∼4.2–300 K.

This way of processing the dependences shown in figure 1 allows one to separate determination of both the total concentration of shallow donor states of impurity phosphorus atoms (N_d) and the total concentration of compensating acceptors (N_a) in non-irradiated and irradiated materials in a quite wide range of doses [11, 12]. This, in its turn, is possible because the degree of compensation (N_a/N_d concentration ratio) is determined by close to the exponential-like ('low-temperature') impurity-ionization region of the $n(1/T)$ dependence, whereas the difference of concentrations ($N_d - N_a$) is obtained by the impurity-depletion ('high-temperature') region (roughly speaking, the $n(1/T)$ dependence shown in figure 1 allows one to solve the system of two equations and find numerical values of N_d and N_a , i.e., the concentration of donors and acceptors).

A decrease in the carrier concentration upon irradiation of n-FZ-Si with 15 MeV protons was found to be due to the occurrence of two processes: (i) a considerable decrease in the concentration of shallow donor states of phosphorus atoms (e.g., due to interaction between impurity phosphorus atoms and mobile vacancies, which results in formation of acceptor-type E-centers) and (ii) comparatively much less or even an insignificant increase in the concentration of radiation-induced acceptors (including the same E-centers, divacancies, etc).

Starting from the foregoing, we estimated the concentration of defects which had taken part in the process of the isochronal annealing using the method of separate determination of the concentrations of the donors and acceptors outlined above; the data are in table 1.

2.2.2. Annealing of irradiated n-FZ-Si material and restoration of electron conductivity. The values of carrier concentration versus the temperature of isochronal annealing are shown in figure 2. The annealing has been carried out in steps of $h_T = 20 \pm 0.5\,^\circ$C with an annealing time at each step of $t = 10$ min.

The stages of annealing shown by vertical lines in figure 2 demonstrate restoring of the donor properties of the dopant. A detailed analysis of these results is beyond the scope of this paper and here we confine ourselves to a summary needed for our further account.

The first stage is attributed to E-centers, which are known to disappear in the temperature interval of annealing ∼100–160 °C [1, 2]. The second stage of annealing in the temperature range ∼180–250 °C is generally accepted to be attributed to the divacancies, (V_2) [13].

The cross section of forming A-centers is smaller by almost an order of magnitude in comparison with the E-centers and, therefore, one can expect a comparatively weak contribution of the concentration of A-centers to the process of annealing [14, 15].

Indeed, the disappearance of the radiation centers within the annealing stage ∼260–280 °C results in supplying a comparatively inconsiderable amount of electrons to the conduction band (whose concentration increases from $\sim 3.8 \times 10^{15}$ cm^{-3} to $\sim 4.3 \times 10^{15}$ cm^{-3} at the stage of annealing under discussion, see figure 2 and table 1). On the other hand, the annealing of the positron-sensitive defects in the interval ∼260–280 °C may be attributed tentatively to A-centers, as they are known to be the positron traps in silicon (in particular, A-centers create shallow positron states [16]).

Table 1. Isochronal annealing of defects in the proton-irradiated n-type FZ-Si.

Type of defects	Defect concentration N (cm^{-3})	Energy level E (eV)	Annealing stage T_{ann} (°C)
E-centers (acceptors)	$\sim(4–5) \times 10^{14}$	$\sim E_c - 0.44$	∼100–160
Divacancies (acceptors)	$\sim 6 \times 10^{14}$	$E_{V2}(-/-) \sim E_c - 0.23$	∼180–250
A-centers (acceptors)	$\sim 5 \times 10^{14}$	$\sim E_c - 0.16$	∼260–280
Deep donors	$\geq 1 \times 10^{15}$	At $E > E_c - 0.24$ eV	∼350–700

The removal rate of electrons from the conduction band ∼110 cm^{-1} for the interval of doses used exceeds the one known for ∼1 MeV electron irradiation by about three orders of magnitude [3]. It is argued that the loss of shallow phosphorus-related donor states is due to interaction of phosphorus atoms with primary defects [17]. As seen from figure 2, the phosphorus-containing centers dominate in restoration of the shallow donor states of the dopant in the course of annealing of the irradiated n-FZ-Si material: subsequently, there have been annealed E-centers, then, probably, the divacancies (V_2) and the defects, tentatively identified as A-centers which disappear in the interval ∼260–280 °C.

The changes of the electron concentration due to isochronal annealing shown in figure 2 demonstrate two salient areas of increase of the electron conductivity, namely, before and after ∼300 °C. The second one is due to recovery of the electrical activity of the phosphorus atoms. In this process the electrons transit to the conduction band from the deep levels belonging to the defects so long as the latter disappear at the comparatively high temperature of annealing, $T_{anneal.} \geq 300$ °C; on this basis (as well by the reason briefly mentioned below) we consider these defects as the radiation centers possessing deep donor levels.

The levels of these defects are not seen in the experimentally obtained $n(1/T)$ dependences in the conditions of our experiments in which the Fermi level changes its position in the course of irradiation and annealing of n-FZ-Si material within the interval $\sim E_c - -(0.21–0.24$ eV). These centers manifest themselves as the positron traps. We will call them in the following as deep donors since the position of the corresponding levels belonging to these centers is, at least, deeper in the forbidden gap than $\sim E_c - 0.24$ eV and because the annealing of these defects results in emission of the electrons to the conduction band which, in its turn, is accompanied with the restoration of the electrical activity of the atoms of dopant.

The defect concentrations given in table 1 were determined from Hall effect measurements over a temperature range of ∼20–300 K for a reference sample irradiated with protons ($D = 8 \times 10^{13}$ cm^{-2}, $E = 15$ MeV) as well as from analysis of isochronal annealing stages. Isochronal annealing of all irradiated samples was carried out in steps of $\Delta T = 20$ °C and $\Delta t = 10$ min. The energy levels of radiation-produced acceptors are well documented in the literature. The identification of A-centers can be considered as tentative, based on the relevant annealing stage. The energy level of deep donors is estimated, taking into account the Fermi level position in proton-irradiated samples at $T \approx 300$ K.

It should be emphasized here that the stages of annealing of the positron lifetime and the stages of annealing detected by electrical and Hall effect measurements are very close to each other, but they do not coincide exactly. In this connection, if this is not specially noticed, we consider throughout the text the temperature intervals of the stages of annealing obtained in the course of the positron annihilation experiments (see e.g., sections 3.9–3.15).

2.3. Positron annihilation lifetime measurements

The positron annihilation lifetime spectroscopic (PALS) measurements were carried out using a conventional fast–fast coincidence system with a high time resolution determined to be 215 ps. The ^{22}Na positron source was sandwiched between two identical 2.5 μm thick Al foils and placed between two identical samples. The samples were etched in CP–4A to eliminate the near-surface damaged region with thickness ∼30–40 μm before measuring the positron lifetime spectra. The samples were isochronally annealed under vacuum conditions for 10 min in steps of 20 K over the temperature range ∼60–600 °C. The samples were cooled down relatively slowly after each annealing step. Between the annealing steps, PALS measurements in the temperature range ∼30–300 K were carried out. Typically, the total number of counts in a single spectrum was 4×10^6. The positron lifetime spectra obtained were analyzed after source and background correction. The source contribution was 10.1%. The spectra were analyzed using two lifetime components which constitute the average positron lifetime via their corresponding intensities I_1 and I_2, i.e. $\tau_{av} = \tau_1 I_1 + \tau_2 I_2$, where $I_1 + I_2 = 1$. The average lifetime is statistically accurate and does not depend strongly on the spectra decomposition.

3. Results

Next we consider the data obtained on the positron lifetime in FZ-Si material before and after irradiation with 15 MeV protons.

A distinguishing feature for the propagation of the positron wave packet in the silicon crystal before its irradiation is that its diffusion length, equal to $l_+ \approx 10^{-5}$ cm in the order of magnitude, is affected by the effective charges of non-covalent bonding of the atoms of residual impurities. In this connection the oxygen-related as-grown centers are of concern, as the concentrations of oxygen and carbon impurities in the investigated material do not exceed $\sim 2 \times 10^{16}$ cm^{-3} and a few 10^{15} cm^{-3}, respectively.

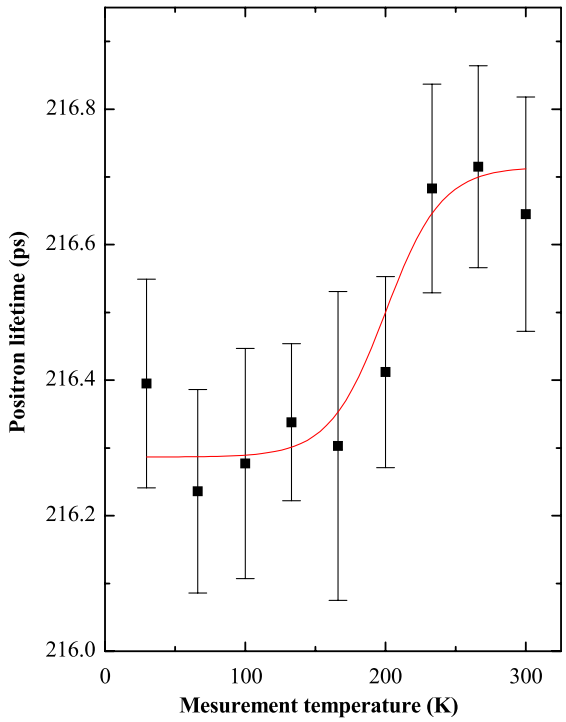

Figure 3. Average positron lifetime versus temperature of measurements in n-FZ-Si ($[P] \approx 7 \times 10^{15}$ cm^{-3}) single crystal. The Boltzmann-like fitted line gives the minimal and maximal values ≈216.26 ps and ≈216.7 ps, respectively; they were used for *a very rough* estimation of the positron binding energy at the shallow traps which are supposedly related to the as-grown oxygen-related complexes (see also figure 4).

After irradiation with 15 MeV protons—even under low doses close to 4×10^{13} cm^{-2}—the pattern of the positron localization changes dramatically to trapping by point defects of a vacancy type. This process dominates up to a surprisingly high temperature (>500–600 °C) of the isochronal annealing of the radiation defects.

3.1. Positron lifetime in n-FZ-Si within the interval ΔT = 30–300 K

The average positron lifetime exhibits a weak non-linear decrease as the temperature goes down from ∼300 to 30 K (figure 3). However, being fitted approximately linearly the experimental data demonstrate the dependency $\tau = \tau_0 + \alpha T$ and the temperature coefficient is $\alpha \approx (16.7 \pm 4.4)$ ps K^{-1}.

Earlier data obtained with worse (lower) resolution $\Delta \sim 232$ ps for an FZ-Si ($[P] = 3 \times 10^{16}$ cm^{-3}) single crystal show a twice as large magnitude of the slope, $\alpha \approx (34 \pm 10) \times 10^{-4}$ ps K^{-1} and such behavior of the temperature dependency of the positron lifetime was attributed to the thermal expansion of the regular lattice of silicon [8]. Below we show that along with this effect, the positron undergoes scattering on the impurity centers in the investigated material: these are the shallow traps where the positron is localized with the binding energy $E_b \geq 0.013$ eV.

Indeed, the positron diffusion constant $D_+ \approx 2.8$–3.1 cm^2 s^{-1} provides a positron diffusion length equal to [9]

$$l_+ \cong \sqrt{D_+ \tau_{av}} \cong 2.46 - 2.6 \times 10^{-5} \text{ cm}, \qquad (1)$$

where the value $\tau_{av} \cong 216.5$ ps of the positron lifetime averaged over the temperature interval ∼300–30 K was used. The average distance between oxygen- and carbon-related centers in n-FZ-Si having concentrations $N_{oxy} \leq 5 \times 10^{16}$ cm^{-3} and $N_{carbon} \approx 10^{15}$ cm^{-3}, respectively, is roughly estimated as

$$R_N^{(\text{oxygen, carbon})} = \sqrt[3]{\frac{3}{4\pi N}} \cong (2.9 - 6.2) \times 10^{-6} \text{ cm}. \qquad (2)$$

The inequality $l_+ \ll R_N$ results in a necessity to take into account the positron interaction with the residual impurities. Below we present some arguments in favor of existing shallow positron states at the as-grown impurity centers that, probably, are characterized by effective exchange with the delocalized states of the thermalized positron.

For simplicity, let the sample, containing the positron weakly bound states at the traps of one kind, be described by the equations of the trapping model connecting the probability of survival (or annihilation) of positrons with the partial positron lifetimes in (i) the completely delocalized states ($\tau \approx \tau_b$), (ii) with the average positron annihilation lifetime τ_{av}, and (iii) with the trapping rate of the positron k into (iv) the weakly bound (shallow) states where the positron lifetime is τ_{st}. For further simplification, we assume that the bulk lifetime is independent of the positron annihilation with the core electrons and, therefore, its value reflects the enhanced density of the bonding electrons around the positron. This approach, known as a two-state trapping model [34], connects the positron trapping rate into the weakly bound states with the average positron lifetime $\tau_{av} = I_{st}\tau_{st} + I_b\tau_b/I_{st} + I_b$:

$$\kappa = \tau_{st}^{-1} \frac{\tau_{av} - \tau_{st}}{\tau_b - \tau_{av}} = \frac{\tau_{st} - \tau_{av}}{\tau_{av} - \tau_b}; \qquad I_{st} + I_b = 1, \qquad (3)$$

where $\kappa \approx \alpha N$, N is the concentration of the trapping centers, $\alpha \cong V/t$ is the trapping coefficient, and V is the volume around the trapping center in which the event of trapping occurs during the time t. If the diffusion of the thermalized positron is characterized quasi-classically by the velocity v_+, then the volume of trapping changes to the positron trapping cross section σ_+ multiplied by v_+, i.e. $V = \sigma_+ v_+$. In this so-called transition-limited regime [9], the positron trapping rate κ competes with the detrapping rate δ since both the delocalized and localized states of a positron in a solid at a temperature T are in thermal equilibrium; according to the principle of detailed balance the ratio δ/κ may be expressed as follows [35]:

$$\kappa = \varphi(T)\delta N \exp[E_b/k_B T] \qquad (4)$$

where $\varphi(T) = (2\pi\hbar/m_+ k_B T)^{3/2}$, E_b is the binding energy of the positron in its weakly bound state ($\hbar$, m_+, k_B are Planck's constant, the positron mass, and Boltzmann's constant, respectively); $\varphi(T) \cong \text{const} \times T^{3/2}$ is a slowly changing function in comparison with the exponential one, so the

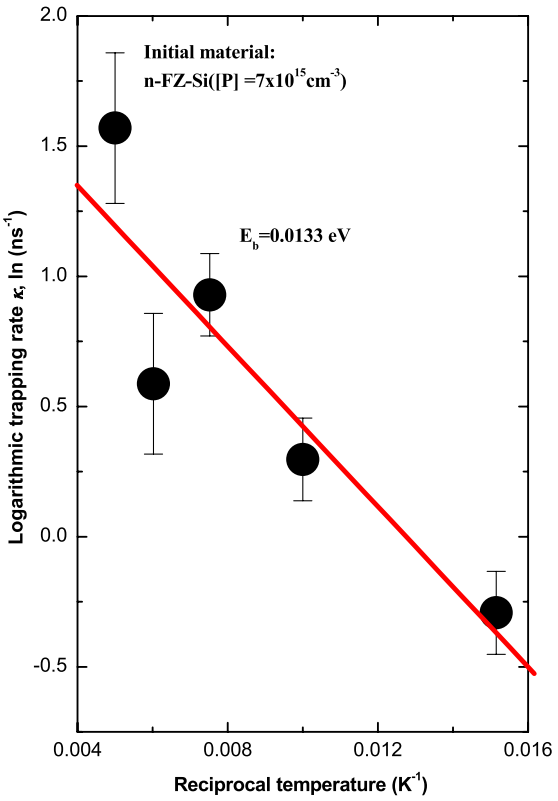

Figure 4. Linearized logarithmic function of the trapping rate (κ) of positrons into the shallow states in n-FZ-Si ($[P] \approx 7 \times 10^{15}$ cm^{-3}) single crystal versus the reciprocal temperature. The positron binding energy at the shallow traps (E_b) is $E_b \approx 0.013 \pm 0.0038$ eV. The line is the result of the linear fitting of the data obtained by equation (5): the correlation coefficient and the standard deviation are ~ -0.9 and ~ 0.36, respectively; the error bars do not exceed $\sim$0.16–0.25, which is the standard error of the mean of the estimated values (i.e. $\sim 0.36/n^{1/2}$, where $n = 5$ is the number of meaningful data points).

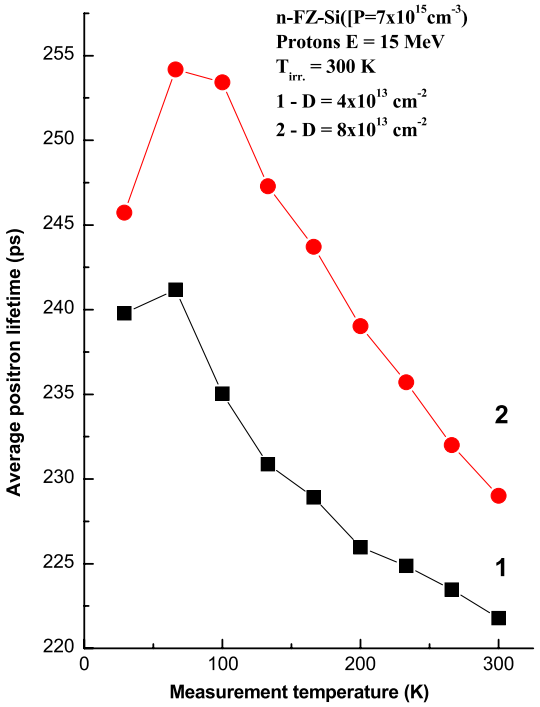

Figure 5. The average positron lifetime versus temperature in n-FZ-Si ($[P] \approx 7 \times 10^{15}$ cm^{-3}) single crystal irradiated with protons, $E_{protons} = 15$ MeV/$T_{irr.} = 300$ K: 1—dose of irradiation 4×10^{13} cm^{-2}, 2—8×10^{13} cm^{-2}. The maximum is due to the shallow positron states formed in the presence of deeper negatively charged positron traps (see section 3.2).

linearized dependency

$$\ln\left(\tau_{st}^{-1}\frac{\tau_{av}-\tau_{st}}{\tau_b-\tau_{av}}\right) = \ln(\text{const.}) + \ln(1/T)^{3/2} + E_b/k_BT \approx C' + E_b/k_BT \quad (5)$$

is to characterize the numerical value of the binding energy of the positron, E_b. Having made inevitable additional assumptions, namely that (i) the positron lifetime $\tau_b(300\text{ K}) \approx 216.7$ ps corresponds to a predominantly delocalized state at room temperature and that (ii) at $T = 0$ K the positron lifetime at the shallow state is equal to $\tau_{st}(0\text{ K}) \approx 216.3$ ps. The latter magnitude corresponds to the crossing of the graph of the extrapolated function of fitting with the ordinate axis at $T = 0$ K (see the fitting line in figure 3); this is a minimal value, which is necessary for the correct use of equation (5).

Obviously, the very rough accuracy of such estimation is due to both smallness and closeness of the nominator to the denominator in the left part of equation (5).

The linearized graph of the function equation (5) for the temperature interval $\sim$66–200 K is shown in figure 4. In spite of a considerable uncertainty caused by the dispersion of the experimental data, the linearity of the graph in figure 4 in itself suggests a qualitative validity of the approach based on the assumption of the existence of occupied weakly bound positron traps: the numerical value of the binding energy ($E_b \approx 0.013$ eV) corresponds to the shallow states. These states should be considered as the states-precursors of the positron trapping by the radiation defects (see sections 3.6 and 3.10).

3.2. Positron lifetime in n-FZ-Si single crystal at different doses of proton irradiation

The primary radiation defects, to be formed along the trajectory of the proton, produce the secondary radiation centers that are considered in this paper. As it has been mentioned above, in section 2.1, the defects influencing the electrical parameters of the material are complexes of vacancies with impurities (e.g., such as E-centers) as well as the multi-vacancy defects of various configurations, including divacancies (see also table 1).

Two different areas are seen on the temperature dependences of the average positron lifetime in the proton-irradiated material (figure 5): under decreasing temperature the average positron lifetime increases over the range $\sim$300–66 K, and then its duration begins to decrease in the interval from the temperature $\leq$100 to $\sim$30 K.

The former reflects the trapping and detrapping of positrons at deeper states (for more details see below, section 3.7). The latter corresponds to the competing process

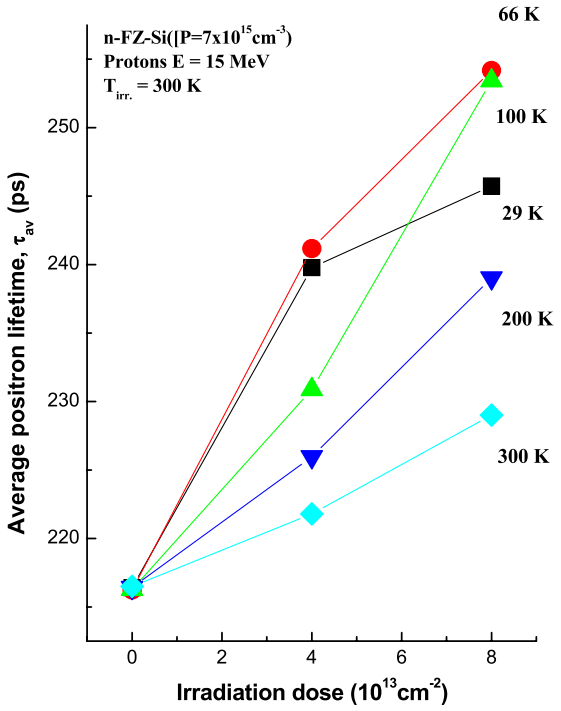

Figure 6. The average positron lifetime at different temperatures in n-FZ-Si ($[P] \approx 7 \times 10^{15}$ cm^{-3}) material irradiated with different doses of protons.

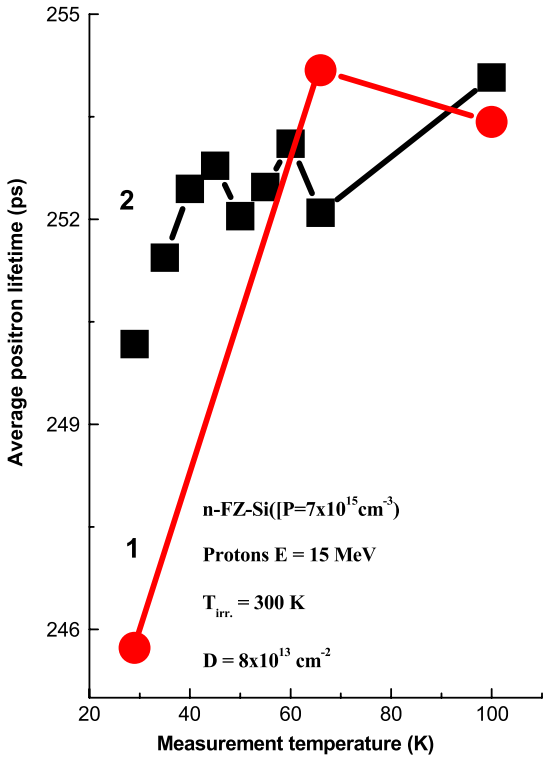

Figure 7. Changes of the average positron lifetime at different temperatures in FZ-Si material irradiated with protons ($E_{\text{protons}} = 15$ MeV/$T_{\text{irr.}} = 300$ K): 1—irradiated material, dose 8×10^{13} cm^{-2} (circles); 2—after the step of isochronal annealing at 60 °C/10 min (squares). The changes observed allow one to associate them to the partial healing of E-centers produced in the course of irradiation. Lines are to guide the eye.

of trapping in which the positrons occupy shallow states where the partial positron lifetime is known to be close to that in the bulk (i.e., $\tau_{\text{st}} \approx \tau_{\text{b}} \approx 216.3$ ps). As a result, the average positron lifetime τ_{av} decreases with temperature over the range from ∼100–66 to ∼30 K when the number of events to be characterized by the value τ_{st} increases. The dependences similar to the ones shown in figure 5 have been analyzed in earlier works concerned with a trapping model that takes into account both shallow and deeper positron traps; comparison of the experimental dependences shown in figure 5 with the ones analyzed in earlier work [9] suggests that the bound energy of positrons at the shallow traps is $E_{\text{st}} \approx 20$–60 meV under the condition that the deeper positron state is related to the negatively charged defect (these results will be discussed in more detail elsewhere).

According to the numerical values of concentrations of the radiation-induced defects (see table 1), a roughly estimated average distance between homogeneously distributed positron traps (N) is $R_N \sim (5–6) \times 10^{-6}$ cm. Inasmuch as $l_+ \sim 2.5 \times 10^{-5}$ cm is the generally accepted value of positron diffusion length in the defect-free bulk of the material (see above, section 3.1), the condition $R_N \ll l_+$ provides the transition-limited regime of the trapping rate of positrons [34]. Also, the positron trapping seems to be far from saturation: indeed, the dependency of the magnitude of the average positron lifetime versus the dose of proton irradiation is close to a linear one over the temperature range ∼30–300 K (see figure 6). Therefore, when the thermalized positron propagates in the bulk of the regular crystal lattice it may occupy either the shallow states produced by the proton irradiation or the shallow states considered above in section 3.1 (and related to the as-grown impurity centers). The shallow states of radiation origin are rather thermally stable during the isochronal annealing and preserved in the material up to the annealing temperature $T_{\text{anneal.}} = 340$ °C (see sections 3.6, 3.7 and 3.10).

3.3. States of positrons trapped by radiation defects in n-FZ-Si: trapping coefficients

The increase of occupancy of the shallow positron traps in passing from higher to lower temperatures ranging from ∼66 to 30 K results in the decrease of the average positron lifetime by ∼10 ps (see figure 7, circles). This magnitude decreases drastically just after the beginning of the annealing process, together with the disappearance of most thermally unstable positron traps (see figure 7, squares). The temperature interval of the changes of the positron lifetime due to isochronal annealing of defects is almost the same as that of E-centers: $\Delta T_{\text{anneal.}} = 60$–180 °C (see table 1).

Estimated by equation (5) the numerical value of the binding energy of positrons at these shallow traps is $E_{\text{b}} \leq 0.01$ eV (see figure 8). As τ_{st} and τ_{b}, parameters of the minimal and maximal values of the average positron lifetime shown in figure 7 (curve 2) were used for the calculations of the κ magnitudes by equation (5). The accuracy of estimation made is rough: the linear fitting of the data in figure 8 gives

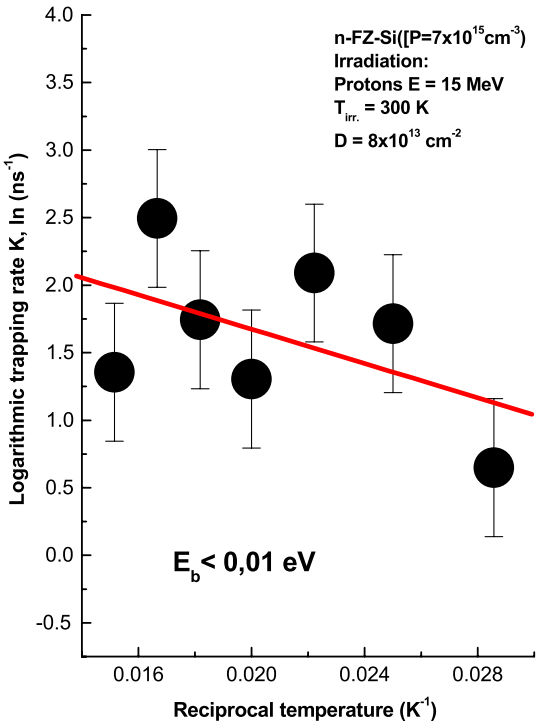

Figure 8. Linearized logarithmic function of the trapping rate κ of positrons into the shallow states in the investigated material of silicon irradiated with protons versus the reciprocal temperature: a very roughly estimated binding energy of positrons E_b is $\leq$0.01 eV; see also equation (5).

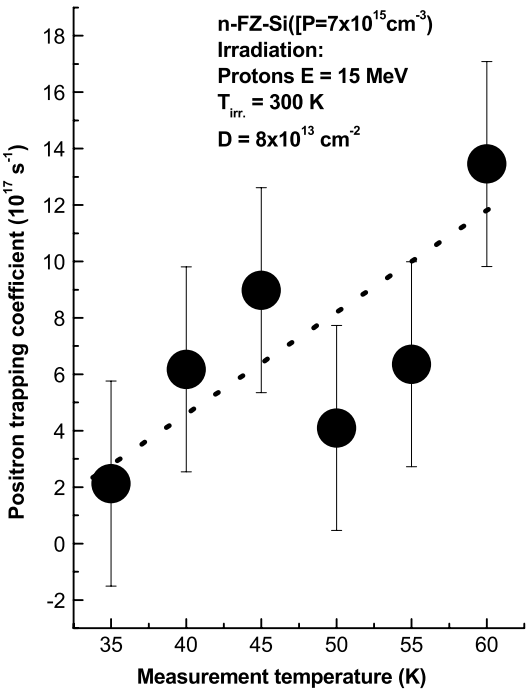

Figure 9. Almost 'gigantic' positron trapping coefficient μ versus measurement temperature: the material after the first step of the isochronal annealing at $T_{\text{anneal.}} = 60\,^{\circ}\text{C}/10$ min. The concentration of E-centers is $\leq 4.5 \times 10^{14}$ cm^{-3} was used for estimations of μ magnitudes. Linear fitting gives values of the standard deviation and the correlation coefficient equal to $\sim$3.2 and $\sim$0.7, respectively.

values of the standard deviation and correlation coefficient equal to $\sim$0.56 and $\sim$0.51, respectively. Interestingly, this result supports the earlier data obtained: in FZ-Si $\langle P \rangle$ single crystal subjected to irradiation with 2 MeV electrons (dose 10^{18} cm^{-2}) comparable numerical values $E_b = 0.048 \pm 0.01$ eV and $E_R = 0.025 \pm 0.008$ eV were found for shallow and the Rydberg positron states, respectively [16]. These data are related to the positron trapping coefficient μ that reflects the positron trapping rate κ per center [9]:

$$\mu = \kappa / c_d, \tag{6}$$

where c_d is the concentration of the centers to be expressed in units of the portion of defects per number of regular atoms in the unit volume of the crystal. Having assumed that E-centers and divacancies dominate in trapping one can obtain the magnitudes of μ equal to 8.4×10^{17} s^{-1} in the proton-irradiated material under investigation (irradiation dose $D = 8 \times 10^{13}$ protons cm^{-2}). This value corresponds to the estimated maximal value of k (100 K) $\approx 1.85 \times 10^{10}$ s^{-1} when the intensity of the long-lived component of the positron lifetime reaches its largest value I_2(100 K) $\approx$ 80% (the parametrized equation (13) was used for the estimation where parameter P_d was accepted to be equal to I_2). The order of magnitude of the positron trapping coefficient $\mu \sim 10^{17}$–10^{18} s^{-1} reflects the numerical values close to gigantic ones which are characteristic of attractive centers of a vacancy type [9, 19]; this range may turn out to be even wider by about an order of magnitude in the case where positron trapping by deep donors is taken into account (see table 1).

As shown in figure 9, the positron trapping coefficient increases over the range $\mu \sim 2 \times 10^{17}$–$1.4 \times 10^{18}$ s^{-1} with decreasing temperature in the interval $\sim$35–60 K: the estimations were made after the first step of the isochronal annealing when E-centers begin to anneal (for certainty, the concentration of E-centers was used for estimations of μ values, see table 1). The range of changes of the positron trapping coefficient is in a qualitative agreement with the prediction that (i) its values may be 'gigantic' ones at very low temperatures and (ii) that the shallow states are involved in the process of the positron localization via the phonon-assisted mechanism [9].

3.4. Estimation of the positron trapping cross section by radiation defects

In a perfect crystal lattice the positron moves as a rather broad packet of waves with the positron thermal wave length L_+ [19]:

$$L_+ \cong h/(3m_+^* k_B T)^{1/2} \approx 50(300\text{ K}/T)^{1/2} \times 10^{-8}\text{ cm}, \tag{7}$$

whose bulk thermal average Boltzmann velocity is:

$$v_+ = (8k_B T_+/\pi m_+)^{1/2} \approx (2.55 k_B T_+/m_+)^{1/2} \approx 9.53 \times 10^6 (T_+/300\text{ K})^{1/2}\text{ cm s}^{-1}. \tag{8}$$

The effective positron temperature T_+ includes zero-point movement; for approximate estimations the temperature

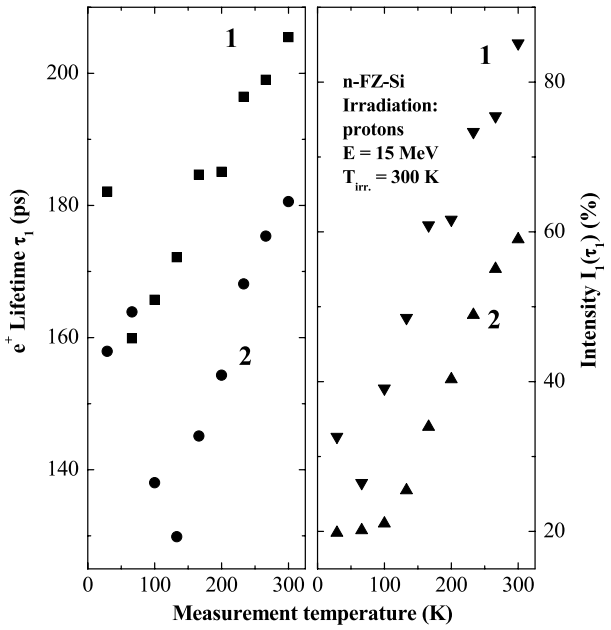

Figure 10. The short-lived component τ_1 and its intensity I_1 versus temperature in n-FZ-Si ($[P] \approx 7 \times 10^{15}$ cm^{-3}) material irradiated with protons, $E_{\text{protons}} = 15$ MeV/$T_{\text{irr.}} = 300$ K: 1—dose of irradiation 4×10^{13} cm^{-2}, 2—8×10^{13} cm^{-2}. The parameters change differently but in parallel with the ones shown in figure 11.

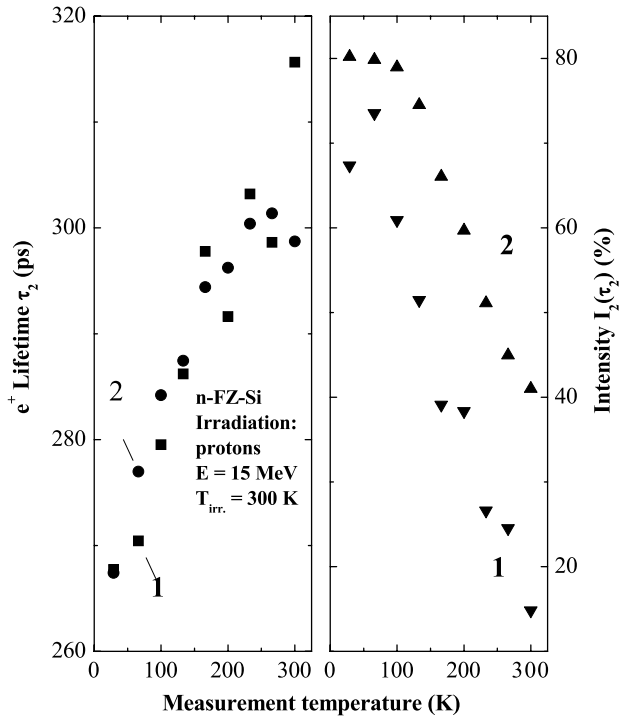

Figure 11. The long-lived component τ_2 and its intensity I_2 versus temperature in n-FZ-Si ($[P] \approx 7 \times 10^{15}$ cm^{-3}) material irradiated with protons, $E_{\text{protons}} = 15$ MeV/$T_{\text{irr.}} = 300$ K: 1—dose of irradiation 4×10^{13} cm^{-2}, 2—8×10^{13} cm^{-2}.

of the crystal is used [34]. As it has been discussed above (section 3.2), in FZ-Si single crystal the diffusion length of the thermalized positron is large in comparison with the average distance between the impurity centers. Under such conditions the positron trapping cross section may be estimated by means of a known concentration of defects c_{d}:

$$\sigma_+ = \kappa / c_{\text{d}} \nu_+. \tag{9}$$

The magnitude of κ in equation (9) characterizes the resulting temperature-dependent positron trapping rate: for estimations of the positron trapping cross section we used the maximal value of $\kappa(100\ \text{K}) \approx 1.65 \times 10^9\ \text{s}^{-1}$, which, in its turn, reflects the high intensity of the long-lived component $I_2(100\ \text{K}) \approx 78\%$. We could estimate the positron trapping cross section σ_+ using parametrized equation (13) where P_{d} is the parameter characterizing annihilation of a positron in its trapped state (see below, section 3.5). Equation (13) underlies much of the research on crystal defects with the positron technique. In particular, the magnitude P_{d} may be determined by means of the values of intensity of the long-lived component I_2 assuming that $P_{\text{d}} \approx I_2$ (in this connection see equation (25) in the work [34] and discussion therein); the values of concentrations of the positron-sensitive defects necessary for estimations are presented in table 1.

We have found that the positron trapping cross section σ_+ ranges from $\sim 12 \times 10^{-13}$ to $\sim 3 \times 10^{-13}$ cm^2. A similar range has been predicted for the attractive centers that trap positrons via shallow (Rydberg) states-precursors into the deeper states [19].

3.5. Estimation of the efficiency of positron trapping in n-FZ-Si irradiated with protons: low doses

An increase of irradiation dose by a factor of two results in a tangible suppression of both the short-lived positron lifetime τ_1 and its intensity (by $\sim$26 ps and $\sim$20%, respectively) whereas the longer positron lifetime τ_2 proves to be independent of the doses of irradiation (compare left parts of figures 10 and 11). An increase of the average positron lifetime with increasing dose of irradiation takes place under one and the same temperature-averaged positron trapping coefficient, $(\langle\mu\rangle^{(2D)}/\langle\mu\rangle^{(1D)}) \approx 1.13$ (the indices $1D$ and $2D$ designate doses of irradiation, 4×10^{13} protons cm^{-2} and 8×10^{13} protons cm^{-2}, respectively).

Indeed, in the case when the production rate of the radiation defects is the same within the considered interval of doses then, according to equation (6), the concentration of defects is

$$c_{\text{d}}^{(2D)} \cong 2 \times c_{\text{d}}^{(1D)} = 2 \times \langle\kappa^{1D}\rangle / \langle\mu\rangle^{(1D)} = \langle\kappa^{2D}\rangle / \langle\mu\rangle^{(2D)}, \tag{10}$$

where the positron trapping rates $\langle\kappa^{1D}\rangle$ and $\langle\kappa^{2D}\rangle$ are averaged over the range of the measurement temperature. Also, we know that the probability to find the positron after its injection into the sample of the irradiated silicon at the moment $t + \text{d}t$ in the bulk is $n_0\,(t)$

$$\dot{n_0}(t) = -(\lambda_0 + \kappa) n_0(t). \tag{11}$$

It is in common use [9] that the positron annihilation rate λ_0 is very close to the one determined for the bulk of the

material before its irradiation, i.e. $\lambda_0 \cong \lambda_b \equiv \tau_b^{-1}$ ns^{-1}. The contribution of this process to the resulting probability of the positron annihilation either in the bulk, P_0, or in the region of defects, $(1 - P_0 = P_d)$ is:

$$P_0 = \lambda_0 \int_0^\infty n_0(t)\,\mathrm{d}t = \frac{\lambda_0}{\lambda_0 + \kappa}, \tag{12}$$

$$P_d = \frac{\kappa}{\lambda_0 + \kappa}. \tag{13}$$

For estimations the magnitude of the bulk lifetime (τ_b) is considered to be the value of the positron lifetime in the interstitial region beyond the defect (a brief discussion of this simplification can be found, e.g., in [9, 34]; starting from this assumption, we further use for numerical evaluations the value $\tau_b^{-1} \cong \langle\lambda_b\rangle \cong 4.62$ ns^{-1} which was determined in the course of investigation of the silicon material before its irradiation with protons, see section 3.1).

Having averaged the intensity I_2 of the long-lived component over the range of the measurement temperature and assuming the validity of equality $\langle I_2\rangle \approx P_d$ one can estimate by equation (13) the magnitudes of $\langle\kappa^{1D}\rangle = 3.65$ ns^{-1} and $\langle\kappa^{2D}\rangle = 8.24$ ns^{-1} which, having taken into account equation (10), immediately give the ratio $\langle\mu\rangle^{(2D)}/\langle\mu\rangle^{(2D)}, \approx 1.13$: it means that the difference between the trapping coefficients obtained for two doses of the proton irradiation used in this work does not exceed ∼13%. Obviously, this result is invariable regardless of using for estimations either the intensity of the long-lived component of the positron lifetime $\langle I_2\rangle$ or the intensity of the short-lived one, $\langle I_1\rangle$.

The closeness of the averaged magnitudes $\langle\mu\rangle^{(1D)}$ and $\langle\mu\rangle^{(2D)}$ may serve as an argument for attributing them to the positron traps of a certain kind. Independently of the dose of irradiation, these traps demonstrate the same rate of decrease of the average positron lifetime with increasing temperature over the range ∼66–300 K (figure 5).

This sameness correlates with invariability of the long-lived positron lifetime with the change of the irradiation dose (figure 11, the left part). Another feature of this kind of trap is that the short-lived component of the positron lifetime becomes shorter (figure 10). The accumulation of these positron traps in the material is accompanied by an increase (decrease) of the intensities of the long-lived (short-lived) components (see the right parts of figures 10 and 11); on the whole, this picture is preserved in the course of the isochronal annealing (see section 4 for more detail).

These regularities reflect the linear dependency (or the one close to it) of the positron trapping rate (κ) on the conditional probability of the annihilation of the trapped positron (P_d/P_0); this linearity takes place for both the interval of the irradiation doses and the range of temperature of measurements. The data speak in favor of the approach based on applying both the value of the average positron lifetime and the intensities of its components for evaluation of the positron trapping rates by equations (14) and (19): we used them for analyzing the results obtained (see below section 4). However, the above-mentioned ∼13% difference between the trapping coefficients obtained for the used irradiation doses

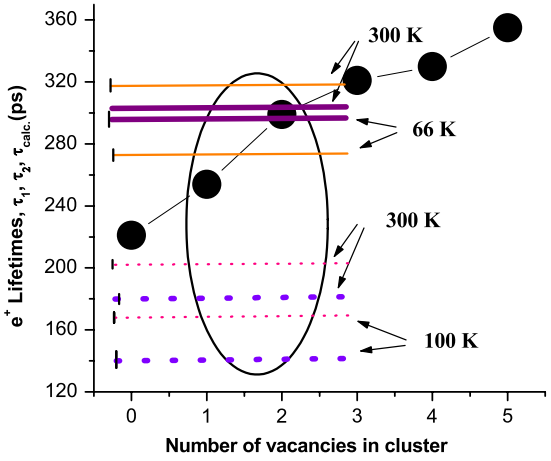

Figure 12. The short- and long-lived positron lifetimes (τ_1 and τ_2) at different temperatures in the proton-irradiated ($E_{protons} = 15$ MeV/$T_{irr.} = 300$ K) n-FZ-Si ($[P] \approx 7 \times 10^{15}$ cm^{-3}) single crystals (lines) versus the calculated positron lifetime for the ideal (unrelaxed) vacancy agglomerates in the neutral charge states (circles) [36]: thin and thick lines correspond to the doses 4×10^{13} protons cm^{-2} and 8×10^{13} protons cm^{-2}, respectively; magnitudes of τ_1 and τ_2 are designated by dotted and solid lines. The ellipse is shown to guide the eye: it includes the vacancy clusters whose free volume corresponds to the values of the positron lifetimes reconstructed by the experimental data. Vertical lines indicate the uncertainty of the values of reconstructed positron partial lifetimes.

reflects a subtle difference in distributions of primary radiation defects produced at random in cascades by protons (this question will be considered elsewhere).

3.6. Binding energy of positron at vacancy-type centers in proton-irradiated n-FZ-Si

The temperature-dependent both short-lived (τ_1) and long-lived (τ_2) positron lifetimes shown in figure 12 are intimately related to the binding energy E_b of positron at the defects of a vacancy type. Their convoluted averaged value $\tau_{av}(E_b)$ is measured versus temperature:

$$\tau_{av} = (\tau_1 I_1 + \tau_2 I_2)/I_1 + I_2 \tag{14}$$

where $I_1 + I_2 = 1$ are the contributions of the short-lived and the long-lived positron lifetimes, respectively. One must obtain the ratio of the positron detrapping rate δ to the trapping rate $\kappa(\tau_{av})$ at different temperatures in order to determine the value of E_b by equation (4). For this purpose it is necessary to express the magnitude κ as a certain function of the average positron lifetime τ_{av} via the steady state equation for the balance of the positron annihilation probabilities:

$$\dot{n_d}(t) = -\lambda_d n_d(t) + k n_0(t), \tag{15}$$

where $n_d(t)$ is the probability to find the positron trapped at the moment $t + \mathrm{d}t$ after its injection into the sample ($\lambda_d \equiv \tau_d^{-1}$ is the positron annihilation rate at the trapped state). The probability to find the positron out of the trapped state $n_0(t)$ at the moment $t + \mathrm{d}t$ is given by equation (11), which is compatible with equation (15).

The contribution of the defect component (P_d), characterizing implicitly the reconstructed intensity of the long-lived component I_2, one may obtain by solving equations (11) and (15) under the boundary conditions $n_0(t = 0) = 1$ and $n_d(t = 0) = 0$, respectively:

$$n_d(t) = \left(\frac{\kappa}{\kappa + \lambda_0 - \lambda_d}\right)\{\exp[-\lambda_d t] - \exp[-(\kappa + \lambda_0)t]\}, \tag{16}$$

$$P_d = \lambda_d \int_0^\infty n_d(t)\,dt = \frac{\kappa}{\lambda_0 + \kappa}. \tag{17}$$

Equations (12) and (17) reflect the fact of a compulsory event of annihilation of a positron either in the defect (s) or in the bulk with the average positron lifetime $\tau_{av} \equiv \lambda_{av}^{-1}$:

$$\tau_{av} = (\tau_0 P_0 + \tau_d P_d)/P_0 + P_d = (\kappa\lambda_d + \lambda_0^2)/\kappa + \lambda_0. \tag{18}$$

The numerical value of the positron trapping rate κ is reconstructed by the parameters of the lifetime spectra by assuming that $\tau_{av} = \lambda_{av}^{-1}$, $\lambda_0 = \langle\tau_b^{-1}\rangle = \lambda_b$, and $\lambda_d = \lambda_2^{min}$ are the magnitudes determined by the experimental data:

$$\kappa = \lambda_0 \frac{\lambda_{av} - \lambda_0}{\lambda_d - \lambda_{av}}. \tag{19}$$

The combination of equations (4), (5) and (19) allows one to evaluate the efficiency of the positron trapping via the positron binding energy E_b at the defect(s):

$$\ln\left(\tau_0^{-1}\frac{\lambda_{av} - \lambda_0}{\lambda_d - \lambda_{av}}\right) \approx C_1 + E_b/k_B T \approx \ln\left\{\lambda_b \frac{\lambda_{av} - \lambda_b}{\lambda_2^{min} - \lambda_{av}}\right\} \tag{20}$$

where $C_1 = C_1' \ln(1/T)^{3/2} \approx$ const is a comparatively slowly changing function.

The binding energy of a positron at the positron-sensitive radiation defects E_b ranges from $\approx$0.0406 $\pm$ 0.005 eV to $\approx$0.07 $\pm$ 0.01 eV with increasing doses of the proton irradiation (figure 13). The interval of the estimated energy values 0.04 eV $\leq E_b \leq$ 0.07 eV includes the characteristic phonon energy $E_{ph} \sim k_B\theta_D \approx 0.056$ eV ($\theta_D = 645$ K is the Debye temperature in silicon). The positron binding energy is affected by the softening [39] of the crystal lattice around the defect of a vacancy type and this factor seems to contribute greatly to the positron trapping/detrapping probability in the phonon-assisted process (see below).

3.7. Positron trapping coefficient for vacancy-type defects and results of ab initio calculations

As shown in figure 14, the character of changes between numerical values of the positron trapping coefficient reconstructed from the experimental data and the ones of calculations [8] in which the positrons were assumed to be trapped from the Rydberg states of large radius into the localized state at the negatively charged vacancies, V^-, is similar. The data for estimations were taken for the sample

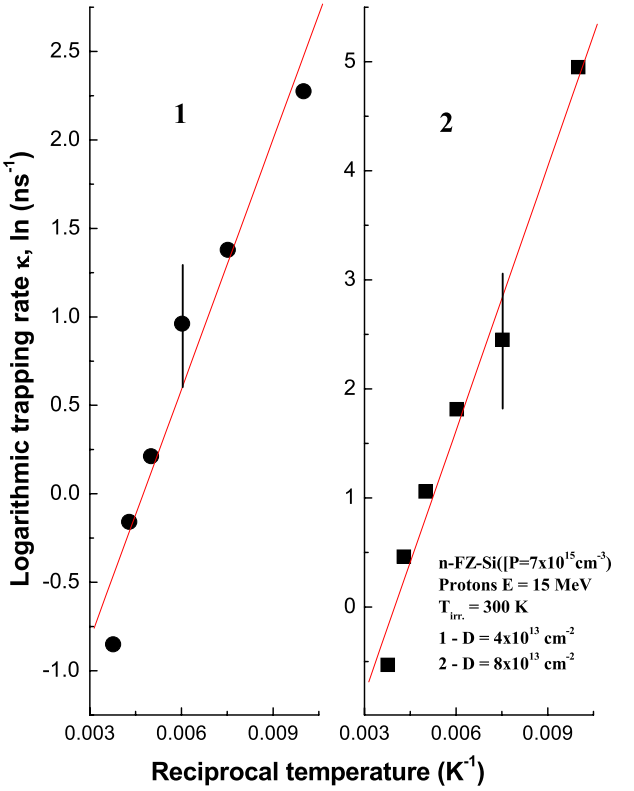

Figure 13. Linearized logarithmic function of the positron trapping rate versus the reciprocal temperature for the radiation centers in the investigated silicon material irradiated with protons; the fitting line corresponds to equation (20): 1—is the binding energy of positron at the radiation defects $E_b \approx 0.0406 \pm 0.005$ eV (the dose 4×10^{13} protons cm^{-2}); 2—$E_b \approx 0.07 \pm 0.01$ eV (8×10^{13} protons cm^{-2}). The positron trapping rate has been calculated by equation (19) using the experimental values of the average positron lifetime τ_{av} obtained within the range ~66–300 K. The standard deviations (the modules of correlation coefficients) were equal to ~0.29(0.97) and ~0.33(0.99) for the data 1 and 2, respectively.

after its isochronal annealing at $T_{anneal.} = 300\,^\circ$C, when most intensive annealing of the deep donors just begins (table 1).

Bearing in mind the difference between real positron traps of the vacancy type and the hypothetical isolated vacancy it would be difficult to expect an exhaustive agreement between experimental and calculated data. Nevertheless, both the value and increase of the positron trapping coefficient μ_+ from $\sim 1 \times 10^{18}$ to $\sim 9 \times 10^{18}$ s^{-1} over the temperature range ~300–66 K suggests intensive interaction of phonons with the positron in the process of its localization.

Disappearance of E-centers and divacancies under the isochronal annealing reduces the numerical value of the positron trapping coefficient. Being estimated for the concentration of deep donors ($N \sim 10^{15}$ cm^{-3}, see table 1) for different temperatures by equation (6) and by equation (19), it varies from $\mu_+(266\text{ K}) \approx 1.1 \times 10^{16}$ s^{-1} to $\mu_+(66\text{ K}) \approx 6.5 \times 10^{17}$ s^{-1} (the temperature dependences of the positron lifetime necessary for the estimations were measured after the isochronal annealing of the irradiated material at $T_{anneal.} = 300\,^\circ$C; for more details see section 4).

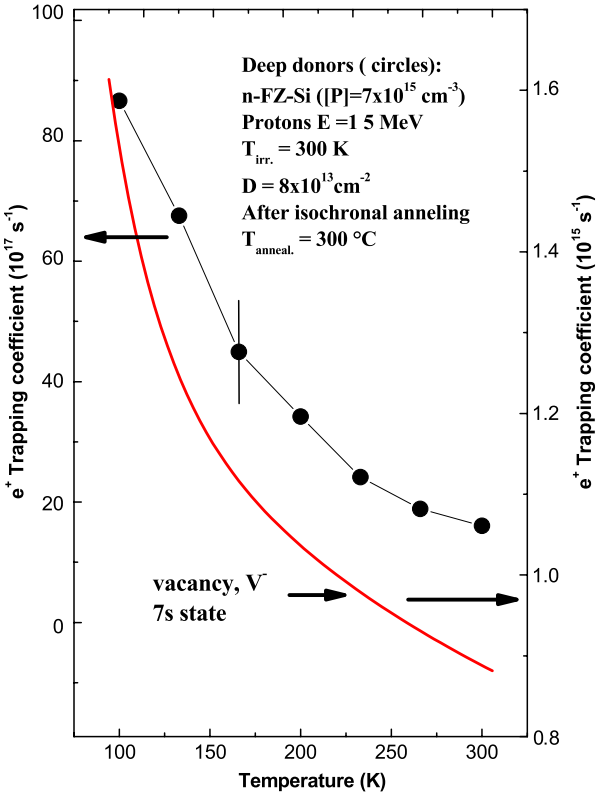

Figure 14. Temperature dependence of the positron trapping coefficient (circles) estimated for the maximal concentration of the deep donors (see table 1) assuming that these defects are the dominating positron traps (approximate accuracy of estimations corresponds to the one of determining the values of concentration). Calculated data (line) for the coefficient of the positron trapping from weakly bound hydrogen-like 7s positron states (Rydberg states) to the localized state at the negatively charged vacancy V^- in silicon were scanned from figure 13 of [4].

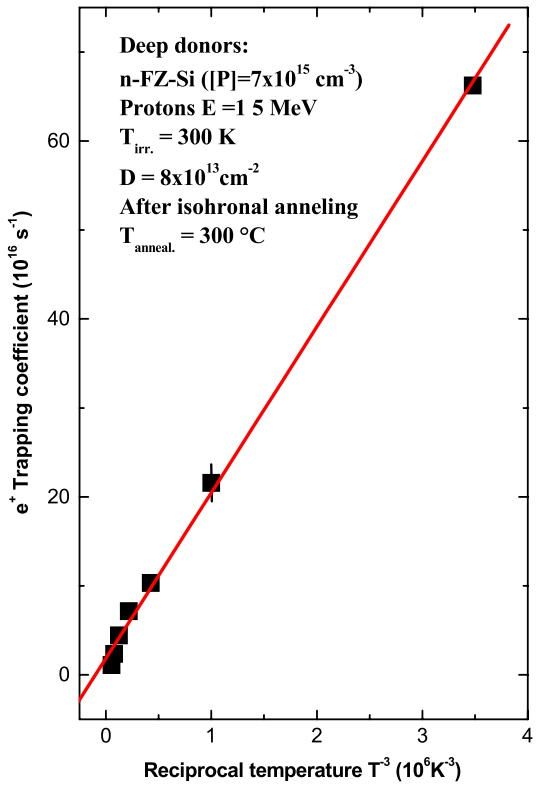

Figure 15. Reciprocal cubic temperature dependence of the positron trapping coefficient (squares) for the deep donors in the proton-irradiated n-FZ-Si. Calculated data (line) corresponds to parameters of the linearized function of equation (21) $A \approx 1.85$ and $B \approx 18.6$ (the correlation coefficient and the mean standard deviation are 0.999 and 0.46, respectively).

The data of investigations of the mechanism of the positron–phonon interaction in the presence of the radiation defects in silicon are scanty [8–10]. Meanwhile, the bulk of evidence on the cascade phonon-assisted process of the trapping of charge carriers by various defects in semiconductors [40] suggests that the trapping cross section is subjected to a general regularity, namely, to a $\sim T^{-3}$-dependency at temperatures $T > 60$ K. Similar regularity has been revealed for the temperature dependency of the positron trapping coefficient under discussion: as shown in figure 15, good agreement of the experimentally obtained μ values to the ones described by equation (21) was found.

3.8. Phonon-assisted cascade positron trapping by defects in proton-irradiated FZ-Si

As seen from figure 15, a strong temperature dependency of the positron trapping coefficient has been obtained in the course of this experiment:

$$\mu(T) \approx A + B \times T^{-3}, \qquad (21)$$

where A and B are slowly changing functions. This dependency describing the experimental data presented in figure 15 is graphic evidence of a cascade phonon-assisted process of the trapping of positrons by the deep donors. The binding energy of the positron trapped at these centers was estimated to be $E_b \approx 0.021$ eV over the range of temperatures from ∼66 to ∼166 K, and this value is lower by $\Delta \sim 0.075$ eV in comparison with the magnitude $E_b \approx 0.096$ eV at higher temperatures, $T > 200$ K (figure 16). This difference in the values of the positron binding energies (figure 16) needs further investigation; to all appearances, it reflects the trapping of positrons into the localized state at higher temperatures from the states of comparatively shorter radius where the positron is bound with an energy ∼0.1 eV in its order of magnitude. It should be recalled that the localized states of positron are characterized by the average positron lifetime $\tau_{av} > \tau_{bulk}$ over the temperature range ∼66–266 K and this inequality includes also the positron partial lifetimes in the states-precursors with respect to the lifetime of a positron in its trapped state (for more details see section 3.1).

The fact of detecting, at least, two magnitudes of the binding energy of the positron at the traps under consideration indicates the existence of a spectrum of the bound positron states which are supposed to serve as precursors for the positron localization at the traps. Both (i) the changes $\Delta E_b \sim 0.075$ eV of the binding energy of the positron at the trap of a vacancy type over the investigated temperature range ∼66–266 K, as well as (ii) the reciprocal cubic temperature

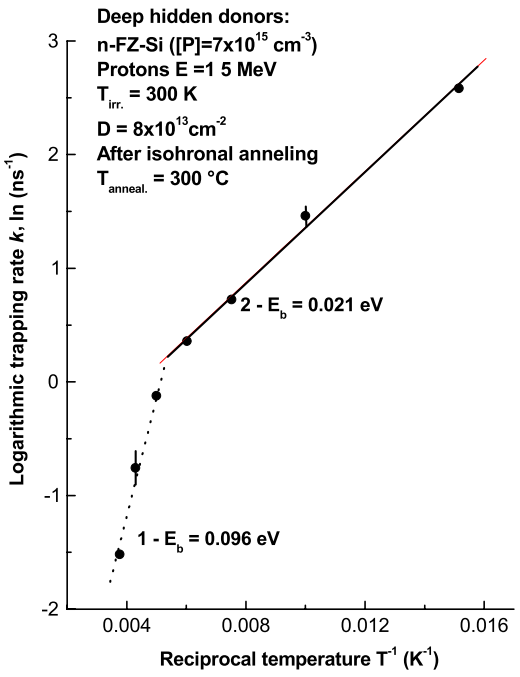

Figure 16. The binding energy of the positron at the deep donor in the proton-irradiated n-FZ-Si single crystal: 1—$E_b \approx 0.096 \pm 0.013$ eV for the temperature interval 200–270 K (dashed line); 2—$E_b \approx 0.021 \pm 0.001$ eV (166–66 K, solid line). Here is plotted the linearized logarithmic function of the positron trapping rate ln κ (circles) versus the reciprocal temperature; the fitting data (line) were calculated by equation (20). The values of κ have been calculated by equation (19) assuming that the maximal experimental value is equal to the lifetime of positron at the defect, $\tau_{max} \cong \tau_d$; as the minimal value we chose the one of the experimental average lifetime at room temperature $T \approx 300$ K, $\tau_{min} \cong \tau_{300\,K}$. The mean standard deviations (the moduli of correlation coefficients) were equal to ∼0.13 (0.99) and ∼0.08 (0.99) for the data 1 and 2, respectively.

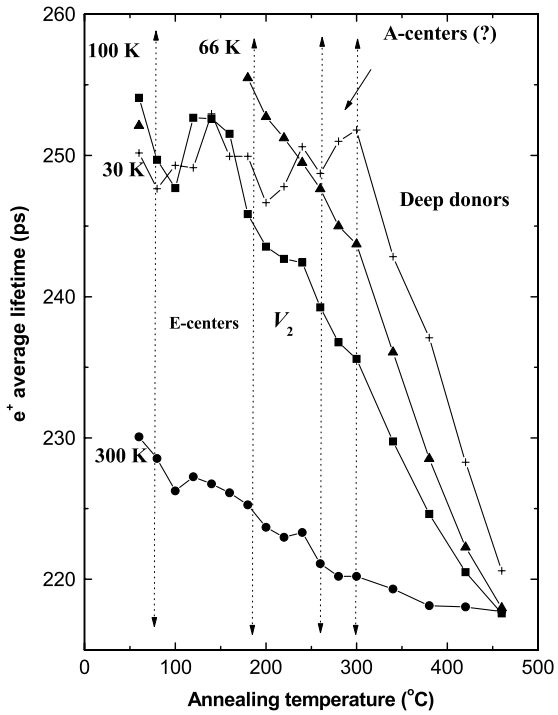

Figure 17. The average positron lifetime versus temperature of isochronal annealing in n-FZ-Si material irradiated with protons, $E_{protons} = 15$ MeV/$T_{irr.} = 300$ K (dose of irradiation is 8×10^{13} protons cm^{-2}), the temperatures of measurements are designated as follows: circles—$T = 300$ K; squares—100 K; up triangles—66 K; crosses—30 K. Approximate intervals of annealing of the *E*-, *A*-centers (tentative attribution), divacancies (V_2), and deep donors are shown by dashed arrows; these intervals correspond to the ones shown by vertical lines in figure 2 (the estimated concentrations of these defects are given in table 1).

dependency of the positron trapping coefficient ($\mu \approx T^{-3}$) substantiate existing multi-phonon cascade emission of positrons in the course of forming the localized positron states at defects of a vacancy type.

3.9. Isochronal annealing of proton-irradiated n-FZ-Si: positron lifetime versus temperature of annealing

Many-staged annealing has been observed: at lower temperatures of measurements (∼30–100 K) two salient ranges of the annealing temperature, before and after ∼250–300 °C, where the average positron lifetime undergoes major changes are seen (figure 17).

We would like to draw the reader's attention to the fact that at higher temperature of annealing, $T_{anneal.} \geq 300$ °C, the range of changes of the lifetime of positrons localized at the thermally stable radiation defects is clearly pronounced under a decrease of the measurement temperature from 300 to 30 K (see figure 17).

As has already been mentioned above, these defects are assumed to be deep donors. For these defects a comparatively strong temperature dependency of the positron trapping coefficient is intimately related to both the positron escape rate from the traps (δ) and the positron trapping rate (κ); see equation (4). A clear correlation between the stages of annealing is observed for both the restored activity of the phosphorus atoms and the changes of the average positron lifetime (see the curves of figures 2 and 17 over the temperature range beyond $T_{anneal.} \geq 300$ °C).

The stages of annealing related to less thermally stable positron traps than the ones associated with the deep donors are also pronounced in the results of the deconvolution of the lifetime spectra obtained at the temperature of measurements $T \approx 66$ K (figure 18). Here the deconvoluted values of both the short-lived and long-lived positron lifetimes converge from their extreme values $\tau_1 \sim 150$ ps and $\tau_2 \sim 275$ ps at the annealing temperature $T_{anneal.} = 300$ °C to a common limit value close to $\tau_{1,2} \sim 218$ ps, thus indicating a return of the positron states to ones characteristic of the initial material at temperatures $T_{anneal.} \sim 460$–500 °C. This result correlates well with the efficiency of restoring the electrical activity of the dopant in the course of annealing of the samples-satellites.

Nevertheless, the restoration of electrical activity of the phosphorus impurity atoms took place up to $T_{anneal.} \sim 700$ °C (see the last stage of annealing on the curve shown in figure 2; these data will be discussed elsewhere in more detail). Rather high thermal stability of the deep donors suggests that they

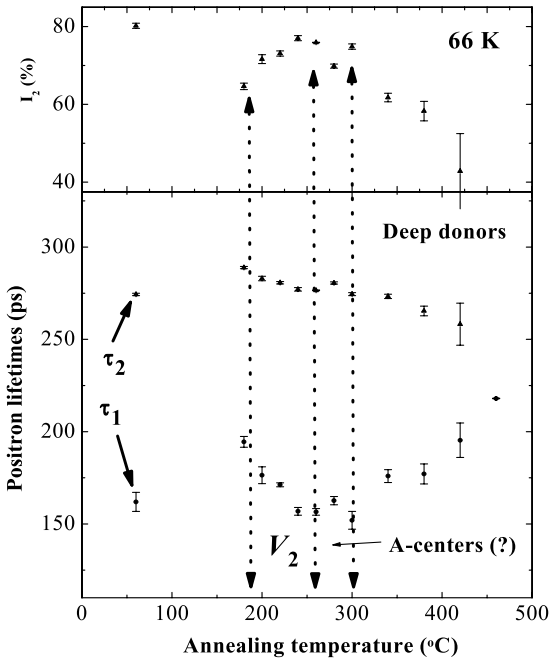

Figure 18. Deconvoluted positron short-lived (τ_1) and long-lived (τ_2) lifetimes versus temperature of isochronal annealing in n-FZ-Si material irradiated with protons, $E_{\text{protons}} = 15$ MeV/$T_{\text{irr.}} = 300$ K, dose of irradiation is 8×10^{13} protons cm^{-2}: the measurement temperature is $T = 66$ K. Intervals of annealing of A-centers (tentative attribution), divacancies (V_2), and deep donors are shown by dashed arrows.

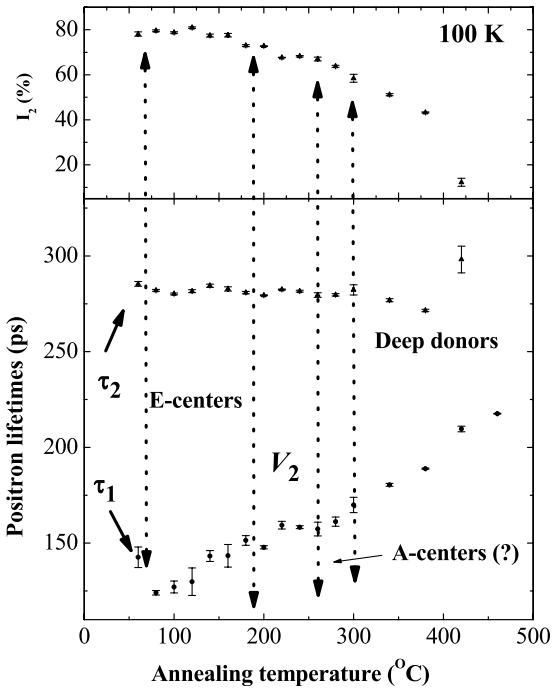

Figure 19. Deconvoluted positron short-lived (τ_1) and long-lived (τ_2) lifetimes versus temperature of isochronal annealing in n-FZ-Si single crystal irradiated with protons, $E_{\text{protons}} = 15$ MeV/$T_{\text{irr.}} = 300$ K (dose of irradiation is 8×10^{13} protons cm^{-2}): the temperature of measurements $T = 100$ K. Approximate intervals of annealing of E-, A-centers (tentative attribution), divacancies (V_2), and deep donors are shown by dashed arrows (the estimated concentration of these centers is given in table 1).

might be hidden within the earlier stages of the isochronal annealing, i.e. at the temperatures $T_{\text{anneal.}} \ll 300\,^{\circ}$C.

It should be noted, however, that at higher temperature of measurements $T \sim 100$ K, the minimal value of the short-lived lifetime, $\tau_1 \sim 125$–130 ps, was observed within the temperature interval of annealing of E-centers at $T_{\text{anneal.}} \approx 80\,^{\circ}$C. These data are in contrast to those obtained at the temperature of measurements $T \approx 66$ K (compare the curves presented in figures 18 and 19). The increase of the short-lived positron lifetime follows the augmentation of the annealing temperature: the stages of annealing attributed to both the divacancies and deep donors are also shown in figure 19. This increase of τ_1 value is accompanied by a decrease of the magnitude of the long-lived component τ_2 as well as its intensity (from the contribution $I_2 \approx 80\%$ up to $I_2 < 10\%$ at the annealing temperature $\geq 500\,^{\circ}$C).

A similar, but less pronounced, picture is observed when the measurements are performed at room temperature (see figure 20). Here are detected the largest magnitudes of the short-lived and long-lived lifetimes, $\tau_1 \sim 175$ ps and $\tau_2 \sim 300$ ps, respectively, under the intensity I_2 (300 K) $\approx 35\%$. The magnitude I_2 (300 K) is suppressed in comparison with that one obtained at $T = 100$ K, I_2 (100 K) $\approx 85\%$ (figure 19). In its turn, this suppression—accounting for the comparatively highest value of the positron detrapping rate at room temperature due, in part, to the increased positron–phonon interaction in comparison with the cryogenic temperatures—results in somewhat weaker changes of the measured average positron lifetime in the course of the isochronal annealing.

3.10. Isochronal annealing of proton-irradiated n-FZ-Si: positron lifetime versus measurement temperature

Last, but not the least interesting (figure 21): there are clearly seen the first, the intermediate, and the last stages of evolution of the temperature dependency of the positron lifetime into the one characteristic of the crystal lattice in the bulk. This may be of paramount importance from the point of view of non-contact/non-destructive characterization of material because the dependency of the average positron lifetime on the measurement temperature manifests itself most observably in the course of the isochronal annealing.

In figure 21 one can see several stages of annealing of the positron traps of the radiation origin whose temperature intervals coincide, approximately, with the ones shown in figures 2 and 17. An almost complete loss of the sensitivity of the average positron lifetime to the positron trapping is observed at a temperature of annealing equal to $\sim 500\,^{\circ}$C, i.e. when a considerable decrease of the concentration of the most thermally stable positron traps of the vacancy type takes place (the activation energy of annealing of these defects is considered below, section 4.4).

As seen in figure 21, two dominating processes of the positron annihilation result in the appearance of a hump on the

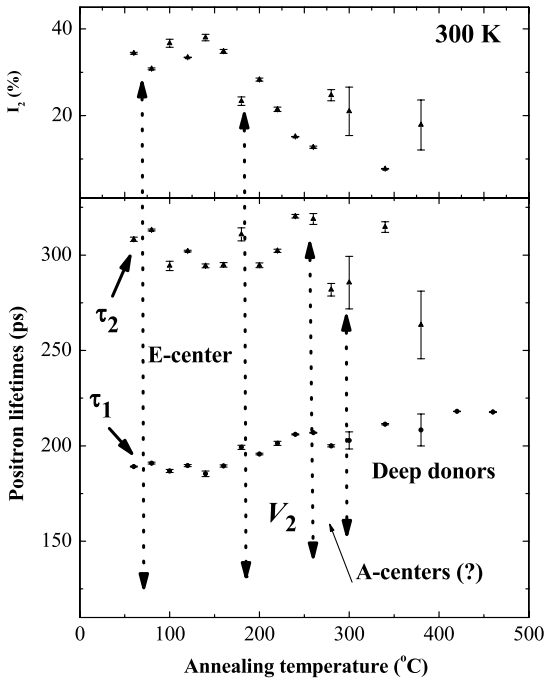

Figure 20. Deconvoluted positron short-lived (τ_1) and long-lived τ_2 lifetimes versus temperature of isochronal annealing in n-FZ-Si single crystal irradiated with protons, $E_{\text{protons}} = 15$ MeV/$T_{\text{irr.}} = 300$ K (dose of irradiation is 8×10^{13} protons cm^{-2}): the temperature of measurements $T = 300$ K. Approximate intervals of annealing of E-, A-centers (tentative attribution), divacancies (V_2), and deep donors are shown by dashed arrows.

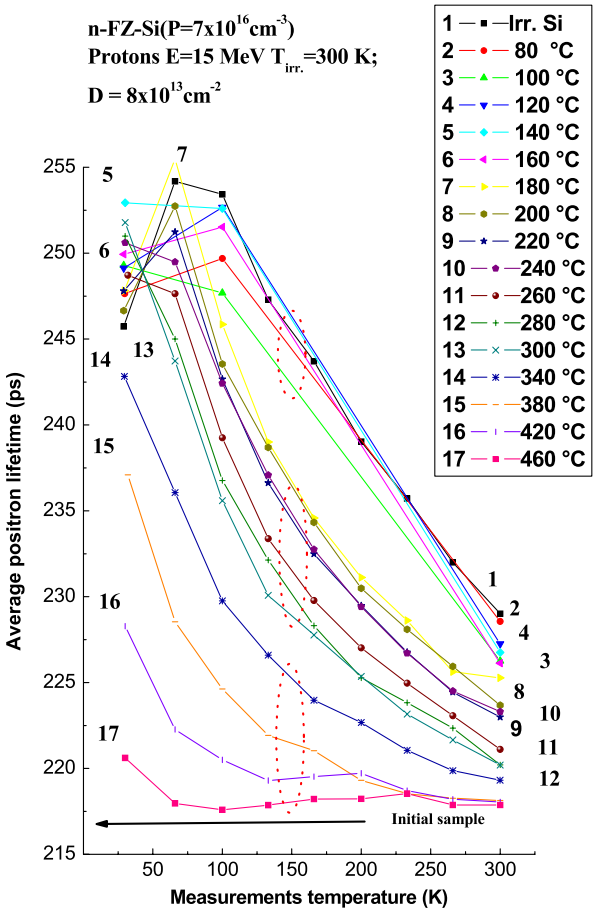

Figure 21. Gradual evolution of the temperature dependency of the average positron lifetime in the process of the isochronal annealing of n-FZ-Si ($[P] \approx 7 \times 10^{15}$ cm^{-3}) single crystal which was irradiated with protons ($E_{\text{protons}} = 15$ MeV/$T_{\text{irr.}} = 300$ K; the dose 8×10^{13} intermediate protons cm^{-2}). Ellipsoids embrace the bunches of curves to guide the eye indicating the first, the intermediate and the last stages of annealing to be discussed in section 4: 1—data for the irradiated material before its annealing; 2—80 °C; 3—100 °C; 4—120 °C; 5—140 °C; 6—160 °C; 7—180 °C; 8—200 °C; 9—220 °C; 10—240 °C; 11—260 °C; 12—280 °C; 13—300 °C; 14—340 °C; 15—380 °C; 16—420 °C; 17—460 °C. The time of annealing was 10 min at each temperature step.

curves of the temperature dependences of the positron lifetime obtained in the course of annealing over the temperature interval ranging from 60 up to ∼300 °C. The first one is related to the shallow (weakly bound) states which are known to demonstrate an increase of the average positron lifetime with the temperature ranging from $T \sim 30$ to $T \sim 70$–100 K. These positron states are confined in a volume of a comparatively large radius. It is argued [34] that they exist at attractive centers having a comparatively small free volume or even when the centers do not have it.

The second process reflects coexistence of both the shallow and localized positron states at an attractive center (see upper and intermediate bunches of curves detailed by ellipsoidal curves to guide the eye in figure 21). Analysis of the competing processes of trapping of a positron into the localized (deep) state via the shallow one having the energy $E_{\text{st}} \approx 20$–60 meV allows us to obtain both the position and shape of the hump (or wide maximum) *similar* to the one which is available on curves 1–10 in figure 21 (for more details see, e.g., [9] and the discussion therein concerning figure 3.13).

For the proton-irradiated n-FZ-Si material under discussion this maximum is observed at somewhat lower temperatures in the interval ∼40–100 K (this maximum is seen in figures 21–25, which present the evolution of defects in the course of the isochronal annealing). The shift of the maximum on the temperature dependency of the positron lifetime indicates a lower binding energy of the shallow positron states in n-FZ-Si material irradiated with 15 MeV protons in comparison with that detected for the positron traps in the electron-irradiated Cz-Si:P single crystal. In both the cases of Cz-Si and FZ-Si materials under consideration the availability of the maximum on the temperature dependences of the positron lifetime is in itself clear evidence of the formation of shallow positron states at the point defects of the radiation origin.

Starting from the foregoing, we can also infer that the competing processes of the trapping and detrapping of positrons by the vacancy-type defects in the proton-irradiated n-FZ-Si ($[P] \approx 7 \times 10^{15}$ cm^{-3}) single crystal result in smearing of the hump on the temperature dependences of the average positron lifetime (see, e.g., curves 1–13 in figure 21).

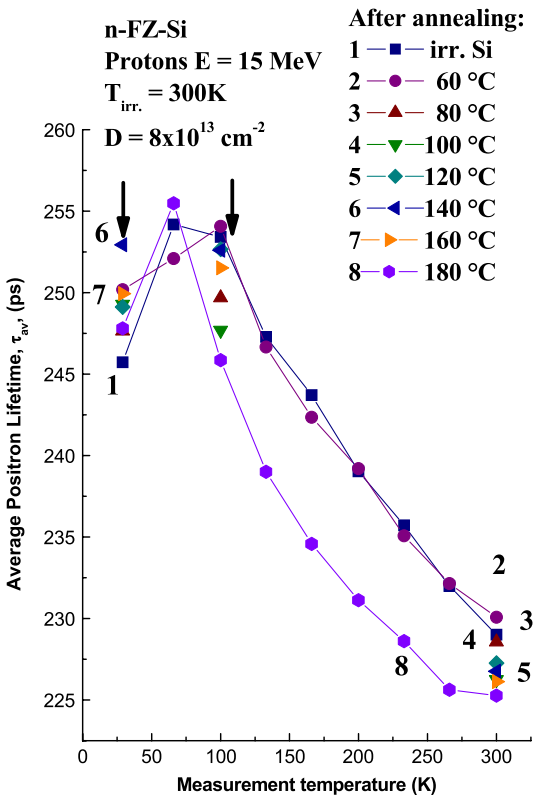

Figure 22. Disappearance of E-centers and the isochronal annealing of the positron traps within the interval $\Delta T \approx 60$–$180\,^{\circ}$C: the average positron lifetime measured at different temperatures in n-FZ-Si material irradiated with protons ($E_{\text{protons}} = 15$ MeV/$T_{\text{irr.}} = 300$ K): 1—the irradiated material, dose 8×10^{13} protons cm^{-2}; 2—after the step of isochronal annealing at 60 °C/10 min; 3—80 °C; 4—100 °C; 5—120 °C; 6—140 °C; 7—160 °C; 8—180 °C. Arrows indicate the temperature interval where comparatively weakly bound (shallow) positron states are markedly competing with the trapping of positrons at the localized states (see text and figure 21 in this connection for more details).

3.11. Annealing of E-centers

Having compared the temperature interval of restoring electrical activity of the phosphorus atoms in the course of the isochronal annealing of E-centers (figure 2) to corresponding interval of changes of the average positron lifetime (e.g., see figure 17) one can notice a close similarity between them, namely, that the range $\Delta T_{\text{anneal.}} = 60$–$180\,^{\circ}$C to be attributed to disappearance of E-centers is clearly seen there in both figures (the estimated concentrations of defects are presented in table 1). At this juncture, during the initial stage of annealing, a marked decrease of the average positron lifetime is observed in the temperature interval ranging from ∼30 to 100 K (figure 22). As has briefly been discussed above, such behavior of the average positron lifetime indicates the existence of the (shallow) state-precursor in which the positron annihilation rate competes with the rate of the positron trapping into the localized state.

The lifetime of the positron in this weakly bound state influences markedly the magnitude of the positron trapping coefficient. The latter begins giving way to the value of positron annihilation rate in the regular lattice below the temperature $T \approx 100$ K, for more details see, e.g., above section 3.8 as well as [8, 9]. To all appearances, the efficiency of forming the weakly bound positron state at the defects of radiation origin in silicon under study is high (mainly, owing to effective phonon-assisted cascade process of the positron trapping discussed above in section 3.8).

The positron-sensitive E-center seems to be not the only defect capable of creating such shallow positron states in the investigated material. The former disappear within the interval ∼60–180 °C, resulting in a partial restoration of the electrical activity of the phosphorus atoms (see figure 2 and/or table 1). The annealing of the E-centers, however, does not lead to a suppression of the components of the positron lifetime spectra to be attributed to the weakly bound positron states. On the contrary, these states demonstrate their thermal stability, manifesting themselves after the annealing of material at $T \approx 180\,^{\circ}$C (see the spectra presented by squares and asterisks in figure 22): a characteristic hump brings in evidence of forming weakly bound (shallow) states-precursors of a positron before its trapping into much more localized state (in more detail these data will be considered elsewhere; see in this connection some earlier findings associated with shallow positron states in various electron-irradiated materials of silicon, e.g., [9, 19, 35]).

The annealing of E-centers results in a tangible decrease of the intensity of the long-lived I_2 positron lifetime component whereas the values of the partial positron lifetimes, both the short-lived (τ_1) and the long-lived (τ_2) ones, heighten markedly: maximal changes Δ of these parameters $\Delta I_2 \approx 16\%$, $\Delta\tau_1 \approx 33$ ps, and $\Delta\tau_2 \approx 14$ ps were found to be the largest for the temperature of measurements $T = 66$ K (see the temperature interval of annealing of E-centers shown in figures 18–20). These changes indicate a decrease of the electron density around the trapped positron (in spite of the increase of the electron concentration in the conduction band after E-centers were annealed, see figure 2): on this evidence, one can state that the positron traps of a vacancy type have a lower electron density contacting the positron and these defects, probably, dominate in the trapping of positrons in the course of annealing.

3.12. Annealing of divacancies

The stage of annealing of defects ranging from 180 to ∼260 °C is generally accepted to be attributed to the divacancies [18]. Their concentration was estimated on the basis of data of electrical measurements and equal to $N_{V2} \approx 6 \times 10^{14}$ cm^{-3} at $T_{\text{anneal.}} = 180\,^{\circ}$C (see figure 2 and table 1).

This attribution may also be based on the numerical value of a positron lifetime ∼250 ps that is close to that evaluated theoretically, namely, ∼254 and ∼299 ps for the unrelaxed neutral vacancy and divacancy, respectively (section 3.6; see also figure 12). The other argument for the identification of these positron traps as divacancies is related to the temperature interval of annealing ∼180–260 °C that was attributed to the motion of these centers during their stress-induced alignment

in the course of experiments on EPR of divacancies created with 1.5 MeV electrons in FZ-Si crystals of p-type [13].

As can be seen in figure 17, a small but marked increase of the average positron lifetime has been observed in the temperature interval of annealing characteristic of divacancies; this increase accompanies the recovery of the concentration of electrons in the conduction band with the magnitude $\sim 2.7 \times 10^{15}$ cm^{-3} (see table 1).

The question whether these positron traps to be attributed to divacancies disappear or they change into traps of a different configuration in the course of annealing requires special consideration. Here it may just be added that within the temperature interval of annealing characteristic of divacancies the intensity of the long-lived component I_2 decreases at the temperature of measurements $T > 100$ K (i.e. in the temperature interval where the weakly bound positron states at the trapping centers are ionized, see figures 19 and 20): the values of decrease are $\Delta I_2(100\ \text{K}) \approx 5\%$ and $\Delta I_2(300\ \text{K}) \approx 15\%$, respectively. This decrease follows the augmentation of the partial positron lifetime: $\Delta\tau_1(100\ \text{K}) \approx 6$ ps, $\Delta\tau_1(300\ \text{K}) \approx 7$ ps, $\Delta\tau_2(100\ \text{K}) \approx 0$ ps, and $\Delta\tau_2(300\ \text{K}) \approx 24$ ps. In contrast, at measurement temperatures $T \leq 66$ K, when the probability of escape of the positron from the trap is comparatively low, I_2 magnitude increases by $\Delta I_2(66\ \text{K}) \approx 11\%$ whereas the values of the partial positron lifetimes become shorter by $\Delta\tau_2(66\ \text{K}) \approx 15$ ps and $\Delta\tau_1(66\ \text{K}) \approx 38$ ps, respectively (see figures 18–20). These changes of the positron partial lifetimes reflect the capture of positrons proceeding in the competing processes via weakly bound positron states discussed above.

At the stage of annealing within the temperature interval ~180–260 °C the weakly bound positron states are still present in the material (see the area of maximum shown by arrows in figure 23). These states compete markedly with the localized ones during the annealing. Apparently, owing to the change of both the concentration and the microstructure of traps, a characteristic hump on the temperature dependency of the average positron lifetime is slightly shifted towards lower temperatures (compare the positions of the area shown by arrows in figures 22 and 23).

Within the narrow temperature range of annealing ~240–260 °C the positron trapping process via the weakly bound state-precursors is effectively suppressed, in which case these states do not result in a pronounced maximum on the graph of the temperature dependency of the positron lifetime (see interval of the measurement temperatures ~30–100 K in figure 23). Even at higher temperatures of annealing, up to ~340 °C, the states under consideration manifest themselves (compare curves 1 and 2 in figure 24): the decrease of the average positron lifetime with the lowering of temperature related to the positron weakly bound states is pronounced at the beginning of the annealing (curve 1), when the concentration of the positron traps is maximal (see, e.g., figure 24 and [9]). Disappearance of the weakly bound states occurs at $T_{\text{anneal.}} > 380$ °C (figure 24) and it accompanies the decrease of the total concentration of the positron-sensitive defects.

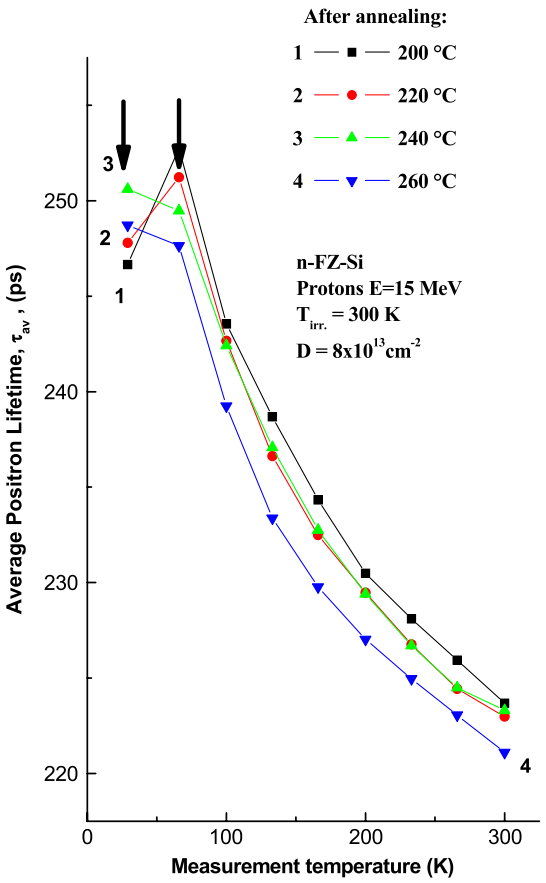

Figure 23. Disappearance of divacancies in the course of the isochronal annealing of the positron traps within the interval $\Delta T \approx 200$–260 °C: the average positron lifetime measured at different temperatures in n-FZ-Si material irradiated with protons ($E_{\text{protons}} = 15$ MeV/$T_{\text{irr.}} = 300$ K, dose 8×10^{13} protons cm^{-2}): 1—after the isochronal annealing at 200 °C/10 min; 2—220 °C; 3—240 °C; 4—260 °C. Arrows indicate the temperature interval where comparatively weakly bound positron states are still competing with the trapping of positrons at the localized states.

3.13. Annealing stage ~260–300 °C: oxygen–vacancy complexes (A-centers?)

This temperature interval of the isochronal annealing is believed to correspond to the beginning of a healing of the oxygen–vacancy complexes including A-centers: see, e.g., the data mainly obtained for Cz-Si crystals where these effects are pronounced [14, 15, 43]. As the isochronal annealing reaches the temperature $T_{\text{anneal.}} \approx 300$ °C, the average positron lifetime in the material under study changes, ranging from ~220 ps at $T_{\text{meas.}} = 300$ K to ~252 ps at $T_{\text{meas.}} = 30$ K (figure 25).

A comparatively insignificant increase of the concentration of electrons in the conduction band (figure 2) correlates with the small (but marked) changes of the average positron lifetime (figure 25) at the same regime of the isochronal annealing (in this connection see also the stages of annealing shown, e.g., in figure 17; see also table 1). It should be stressed that the attribution of the interval of annealing ~260–300 °C to both A-centers and other

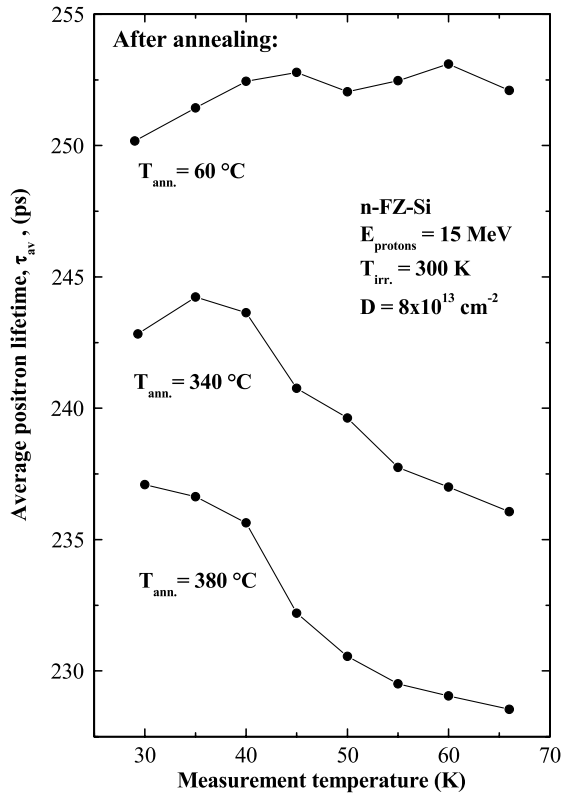

Figure 24. Thermal stability of weakly bound positron states at the radiation defects competing with the trapping of positrons at the localized states. Here are shown the data obtained after the first step of isochronal annealing at 60 °C/10 min and at the end of the process of annealing of the shallow traps (at 340 °C and 380 °C, respectively).

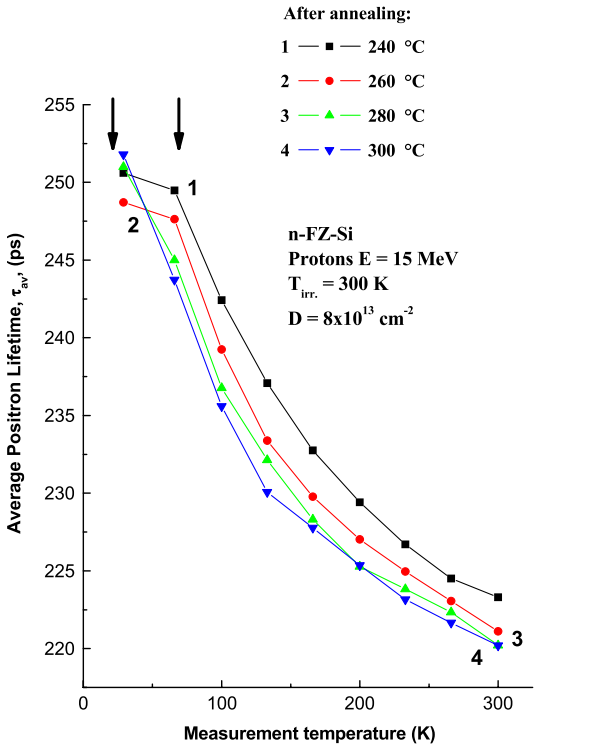

Figure 25. Disappearance of the oxygen-related positron traps of radiation origin (supposedly, A-centers), and the isochronal annealing of the positron traps within the interval $T_{\text{anneal}} \sim 240$–$300\,^{\circ}\text{C}$: the average positron lifetime measured at different temperatures in n-FZ-Si material irradiated with protons ($E_{\text{protons}} = 15$ MeV/$T_{\text{irr.}} = 300$ K, dose 8×10^{13} protons cm^{-2}): 1—after the isochronal annealing at 240 °C; 2—260 °C; 3—280 °C; 4—300 °C. Arrows indicate the temperature interval where the weakly bound positron states are still markedly competing with the trapping at the localized states (see also this area shown by arrows in figures 21–23).

(obviously, available) oxygen-related centers using the data obtained may be just tentative at this stage of studying of the proton-irradiated n-FZ-Si material.

3.14. Annealing of deep donors at $T_{anneal.} \geq 300\,^{\circ}C$

A main feature of the isochronal annealing of the radiation defects under investigation within the temperature interval ∼60–300 °C is that the disappearance of the positron traps does not affect essentially the average positron lifetime (figure 17) whereas the restoration of a considerable amount of electrons in the conduction band in this temperature range has been observed (figure 2).

3.14.1. Comparison of data of electrical and positron annihilation measurements. For the stages of annealing discussed above in sections 3.11–3.13 a total increase of the concentration of conduction electrons in the investigated material is $\sim(1.4\text{–}2) \times 10^{15}$ cm^{-3} (table 1). Further annealing of the positron-sensitive defects occurs, probably, under lower rate of restoring the donor activity of the atoms of dopant; however, during this annealing stage there has been observed the most marked disappearance of the positron traps manifesting themselves as deep donor centers.

The defects possessing properties of deep donors seem to be hidden from detection by the low-temperature electrical measurements during earlier stages of isochronal annealing at $T_{\text{anneal.}} \leq 300\,^{\circ}\text{C}$ (see figure 2). On the contrary, comparatively *slow* restoration of the positron annihilation parameters at the temperatures $T_{\text{anneal.}} \leq 300\,^{\circ}\text{C}$, is in itself a fact suggestive of forming the deep donors under discussion in the course of irradiation (see, e.g., figure 26).

The question about the process of formation of deep donors requires further investigation; anyway, being an effective positron attractor, it is this center of radiation origin that dominates in the process of annealing at temperatures higher than $T_{\text{anneal.}} \geq 300\,^{\circ}\text{C}$.

As seen in figure 26, both the long-lived partial positron lifetime (τ_2) and corresponding intensity (I_2) decrease most considerably following the annealing at $T_{\text{anneal.}} > 300\,^{\circ}\text{C}$; accordingly, the short-lived positron lifetime (τ_1) increases from its minimal value ∼150 ps at $T \approx 300\,^{\circ}\text{C}$ to the magnitude ∼212–218 ps at the end of the annealing process to be detected by means of the positron lifetime spectroscopy. Simultaneously with these changes of the positron trapping by the deep donors, in the temperature range ∼300–600 °C a large portion of the phosphorus atoms regain their own

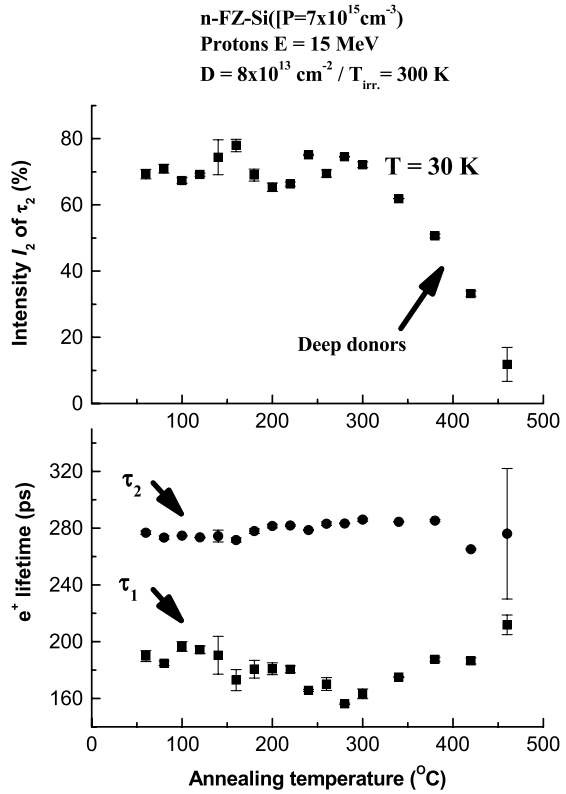

Figure 26. Deconvoluted long-lived (τ_2, I_2) and short-lived (τ_1) positron lifetime components versus temperature of the isochronal annealing in n-FZ-Si material irradiated with protons, $E_{\text{protons}} = 15$ MeV/$T_{\text{irr.}} = 300$ K, dose of irradiation is 8×10^{13} protons cm^{-2}; the measurements of the average positron lifetime were performed at $T \approx 30$ K. For the chosen steps of isochronal annealing the positron lifetime is beginning to recover at $T_{\text{anneal.}} \sim 300\,^{\circ}$C. Within the interval ∼300–500 °C the isochronal annealing results in almost complete restoration of the average positron lifetime value which is characteristic of the bulk material (∼216.5 ps). This temperature interval corresponds to the annealing of the deep donors whose concentration was *roughly* estimated to be equal to $\sim 10^{15}$ cm^{-3} (see table 1).

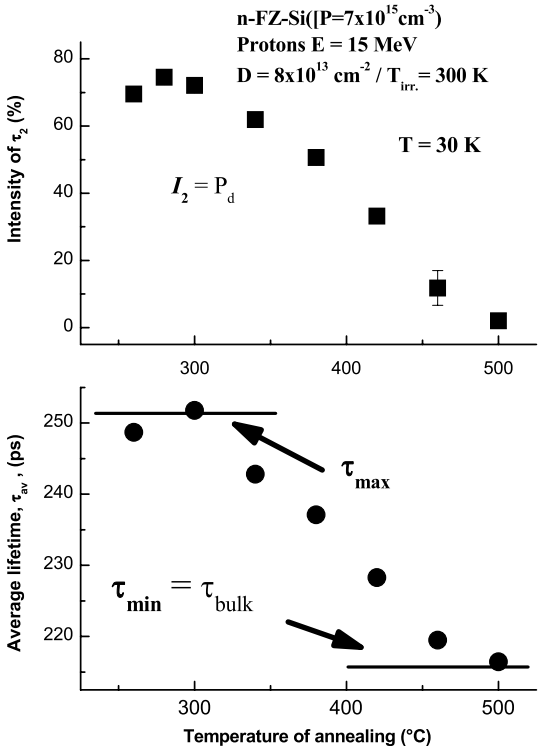

Figure 27. The intensity of the long-lived component and the average positron lifetime within the temperature interval of the annealing of the deep donors in the investigated material. The minimal and maximal values of the average positron lifetime τ_{av} have been applied for estimation of the activation energy of annealing of the positron traps by equation (26). For the calculations of the positron trapping rate κ_i at each step of annealing, equations (17) and (19) were used, assuming that $I_2 = P_{\text{d}}$, $\tau_{\text{max}} = \tau_{\text{d}}$, and $\tau_{\text{min}} = \tau_{\text{b}}$.

electrical activity (compare curves shown in figure 2 with the ones of figure 26).

Over the range of temperature $\Delta T_{\text{anneal.}} \geq 460$–$480\,^{\circ}$C, when a considerable amount of deep donors are annealed, the sensitivity of positrons to the trapping by these defects decreases dramatically. The contribution of the long-lived component I_2 becomes almost negligibly small; the average positron lifetime reaches a value which is close to that found for the initial non-irradiated material, ∼216.5 ps (figure 27). However, the results of electrical measurements are still demonstrating the restoration of the electrical activity of dopant up to $T_{\text{anneal.}} \approx 660$–$680\,^{\circ}$C (figure 2).

Thus, a good correlation between the data of the electrical measurements and the positron lifetime spectroscopy on the isochronal annealing substantiates the identification of the deep donors as the positron-sensitive vacancy complexes whose microstructure involves, presumably, at least, one vacancy and a phosphorus atom; it goes without saying that these defects are not E-centers, which have already been completely annealed.

3.14.2. Annealing of deep donors as a quasi-chemical reaction: estimation of activation energy. Rather monotonous changes of the average positron lifetime within the temperature interval ∼300–500 °C allow one to estimate the activation energy of annealing on the basis of the assumption that this process proceeds under one value of the activation energy.

In this event the rate of annealing of defects is described by the diffusion equation [45] which is characterized by the energy of activation barrier E_{a}:

$$\mp \frac{\mathrm{d}N_{\text{d}}}{\mathrm{d}t} = f(N_{\text{d}}) \times C \equiv f(N_{\text{d}}) \times C_0 \exp\left(-\frac{E_{\text{a}}}{k_{\text{B}}T}\right), \quad (22)$$

where $f(N_{\text{d}})$ is continuous function of the concentration of defects (N_{d}), C is a characteristic kinetic coefficient, and C_0 is a constant (a minus sign corresponds to a decrease of the concentration of defects). When $f(N_{\text{d}})$ is a certain power function of N_{d}, then equation (22) becomes the equation of the chemical kinetics:

$$\mp \frac{\mathrm{d}N_{\text{d}}}{\mathrm{d}t} = CN_{\text{d}}^{\gamma} = N_{\text{d}}^{\gamma} C_0 \exp\left(-\frac{E_{\text{a}}}{k_{\text{B}}T}\right), \quad (23)$$

where E_{a} and γ are the activation energy of the annealing process and the parameter determining the order of reaction,

respectively. The latter, on the whole, indicates the number of different types of defects to be annealed [45]. In the practically useful simplification, equations (22) and (23) both describe the annealing process as a quasi-chemical reaction, in which case the stepwise change of temperature in the course of the isochronal annealing may be changed to a constant rate of heating, i.e. $T = \alpha t$, where t and α are the time elapsed since the beginning of the annealing and the rate of heating, respectively. Then one can use a new variable in equation (22):

$$\mathrm{d}N_\mathrm{d}/f(N_\mathrm{d}) = -C_0\alpha^{-1}\exp\left(-\frac{E_\mathrm{a}}{k_\mathrm{B}T}\right)\mathrm{d}T. \qquad (24)$$

Having changed $f(N_\mathrm{d})$ to N_d^γ in equation (24) one can get the function

$$(-\mathrm{d}N_\mathrm{d}/\mathrm{d}T_\mathrm{a}) = K_0\alpha^{-1}N_\mathrm{d}^\gamma\exp(-E_\mathrm{a}/k_\mathrm{B}T_\mathrm{a}) \qquad (25)$$

where $T_\mathrm{a} = at$ is the temperature of annealing, $a \approx \alpha$ is the averaged rate of heating ($-a \approx (T_i - T_{i+1})/t_h = h/t_h$, where h and t_h are the constant temperature step and the time of annealing at each step, respectively). It is usually assumed that one can separate the variables in equation (25), i.e. $N_\mathrm{d}(T, t) \cong N_\mathrm{d}(T)$. This assumption allows one to estimate an approximate magnitude of the activation energy of the process of annealing, E_a, that characterizes the dynamics of the component parts of the defects to be annealed.

For the estimations of E_a values we used the maximal positron trapping rates that were calculated on the basis of the positron lifetime measurements at $T_\mathrm{meas.} = 30$ K. The positron traps are supposed to disappear (i) with constant activation energy E_a; the other assumption is that (ii) equations (6), (9), (14), (17) and (19), connecting proportionally the positron trapping rate κ_i and the concentration of defects, are justifiable in the whole range of the annealing temperatures. The numerical value of κ_i was established to be proportional to the concentration of defects within the interval of the irradiation doses $\sim(4\text{–}8) \times 10^{13}$ protons cm^{-2} for the whole temperature range of measurements ~30–300 K. This proportionality underlies the substitution $N_\mathrm{d} \approx c_1 \times \kappa$; where $c_1^{-1} \approx \sigma_+ \times v_+$ (σ_+ and v_+ are the positron trapping cross section and the velocity of thermalized positron, respectively).

Also, we assume that (iii) the coefficient K_0 in equation (25) is proportional to the diffusion coefficient of the defect whose disappearance in a sink is not accompanied by the formation of any other defects contributing to the positron trapping rate. For homogeneous distributions of both the positron traps and sinks (iv) equation (25) gives a linearized function $\varphi(T_\mathrm{a})$ whose slope determines the value of the activation energy E_a:

$$\varphi(T_\mathrm{a}) = \gamma\ln\kappa - \ln(\mathrm{d}k/\mathrm{d}T_\mathrm{a}) = A + E_\mathrm{a}/k_\mathrm{B}T_\mathrm{a}, \qquad (26)$$

where $\gamma = 1$ is for the first order of the reaction that, in its turn, corresponds to the conditions (i)–(iv) mentioned above. The linearized function φ ($\gamma = 1$, T_a^{-1}) is shown in figure 28; for the calculation of the positron trapping rate κ_i both the values of the average positron lifetime and the intensity of the long-lived component obtained at the temperature $T \approx 30$ K were used.

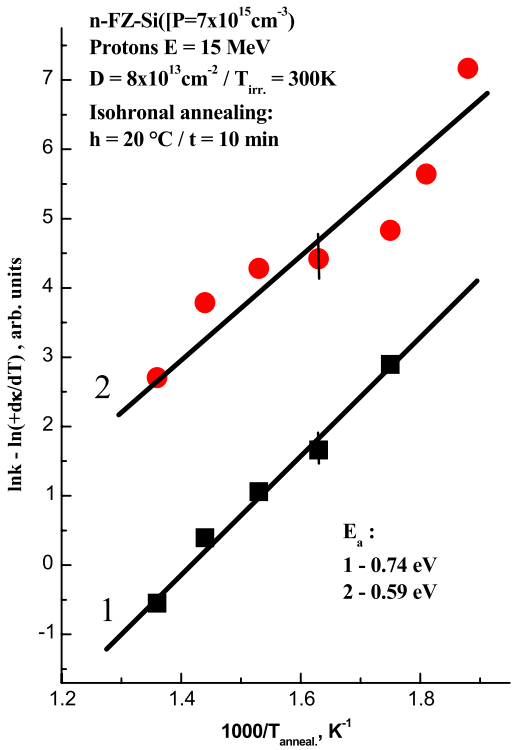

Figure 28. The annealing of deep donors at the last stage ($\Delta T_\mathrm{a} \sim 300\text{–}500\,^\circ$C) in n-FZ-Si ($[P] \approx 7 \times 10^{15}$ cm^{-3}) single crystal irradiated with 15 MeV protons ($D = 8 \times 10^{13}$ protons cm^{-2}, $T_\mathrm{irr.} = 300$ K): 1—the activation energy of annealing $E_\mathrm{a} \approx 0.74$ eV; 2—$E_\mathrm{a} \approx 0.59$ eV. The first order of reaction is observed; the squares and solid line are the experimental and calculated data obtained by equation (26) using equations (19) and (17) for calculations of the positron trapping rate κ_i (lines 1 and 2, respectively). The mean standard deviations (the modules of correlation coefficients) were equal to ~0.17 (0.99) and ~0.54 (0.94) for the data 1 and 2, respectively.

As seen from figure 28 (line 1), the experimental data are close to the fitting function obtained for the activation energy $E_\mathrm{a} \approx 0.74$ eV when the positron trapping rate κ_i was determined using equation (19) based on the measurements of the average positron lifetime (section 3.7; the parameters λ_b, λ_d are obtained by experimental data having assumed, in particular, that $\lambda_\mathrm{d} \approx \tau_\mathrm{av}^{-1}(\mathrm{max})$ is a minimal value over the range of the positron lifetime temperature measurements and λ_b is the positron lifetime in the bulk).

Another numerical value $E_\mathrm{a} \approx 0.59$ eV has been obtained when for calculations of the positron trapping rate the parametrized equation (17) is used, see the data points and the fitting line (2) in figure 28. It is known that equation (17) underlies much of the research on crystal defects with the positron technique. In particular, the P_d value may be determined by the intensity of the long-lived component I_2 assuming that $P_\mathrm{d} \approx I_2$, in this connection see equation (25) in [34] and the discussion therein.

Within the framework of the assumptions made, the values of the activation energy (≈0.59 and ≈0.74 eV) should be considered as the ones close to each other. We would like to draw the reader's attention to the fact that the magnitudes within the interval of energies ~0.25–0.45 eV has been

much discussed in connection with the problem of the energy of dissociation of vacancy–phosphorus atom complexes in silicon (for more details see [1, 39]); also, the energy ≈1.3 eV was estimated to be the activation energy for diffusion of divacancies in EPR experiments [13]. Bearing in mind the roughness of the assumptions made we consider the values $E_a \approx 0.59$ and 0.74 eV as approximate ones that, nevertheless, are common with the dynamics of the point radiation centers of a vacancy type in silicon.

Starting from the foregoing, one can suggest that the process of annealing to be characterized by the first order of the quasi-chemical reaction contributes considerably to dissociation of the positron traps. This process accompanies the restoring of the electrical activity of the phosphorus atoms. The rate of annealing at the last stage, to all appearances, depends only on the concentration of defects of the one type, and it is this process that results in dissociation of the deep donors. For these defects a large magnitude of the positron trapping coefficient μ changing from $\sim 10^{16}$ to $\sim 7 \times 10^{17}$ s^{-1} within the temperature interval ∼30–300 K has been found (see above, e.g., figure 15 and text in section 3.8).

Only one stage of annealing of the deep donors has been revealed over the temperature range ∼300–500 °C; nevertheless, we cannot exclude other scenarios of annealing that may depend on the doses of proton irradiation.

Inasmuch as the probability of the positron trapping by the defects under study is not measured directly, its value depends on the method of calculation of the positron trapping rate [46]. The latter is intimately related to the range of changes of the magnitudes of both the positron lifetimes (τ_{av}) and the intensity (I_d) of the long-lived component [47]. This range determines slightly different changes of the positron trapping rate to be calculated by equation (17) and by equation (19); finally, the difference $\sim \Delta E_a \approx 0.15$ eV appears (one should consider numerical values of E_a as the limiting ones obtained at lowest temperature of measurements $T_{meas.} \approx 30$ K).

3.15. Positron lifetime and number of vacancies involved in deep donor

Last, let us compare the average positron lifetime magnitudes attributed to the deep donors with the data of *ab initio* calculations of the lifetimes of positrons localized at the multi-vacancy complexes (see figures 12 and 29).

First of all, we must notice the very close values of the measured and calculated positron lifetimes that correspond to the number of vacancies $1 \leq n \leq$ (2–3), see figure 29. Taking into account the inward relaxation in the calculations of the positron lifetime in the vacancy clusters just refines this inequality, namely $n \leq 2$ (in this connection see also [9, 37, 38] where a brief discussion on what the value of the positron lifetime might be for the divacancy is given). It should be stressed that both the number of vacancies and values of the positron lifetime obtained for the deep donors are close to those registered for the irradiated material before its annealing (see figure 12). It means that during the total interval of annealing positrons are trapped by the point defects

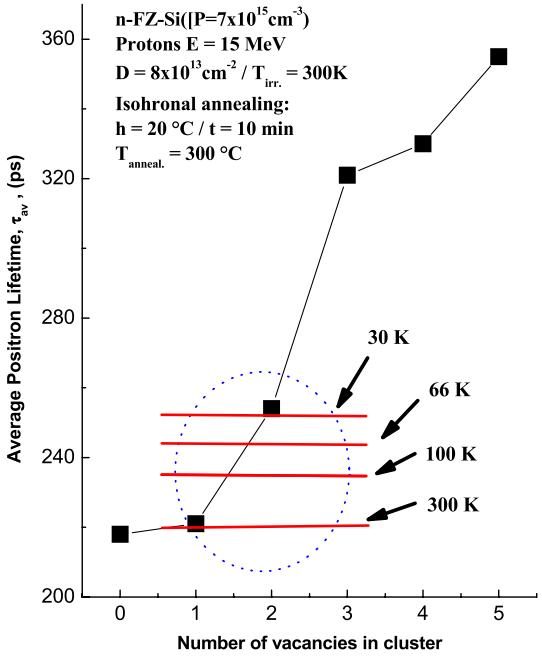

Figure 29. The number of vacancies in the microstructure of the deep donors in the proton-irradiated n-FZ-Si ($[P] \approx 7 \times 10^{15}$ cm^{-3}) single crystals after the step $T_{anneal.} \sim 300$ °C of isochronal annealing ($E_{protons} = 15$ MeV/$T_{irr.} = 300$ K): the lines designate the average positron lifetimes τ_{av} measured at different temperatures. The calculated positron lifetime values (squares) for the ideal (unrelaxed) vacancy agglomerates in the neutral charge states are cited by [36]. The ellipsoidal curve is shown to guide the eye: it includes the number of vacancies whose free volume corresponds to the lifetimes observed.

of a vacancy type (i.e. not by the multi-vacancy clusters) and it is this process that dominates.

The consequent disappearance of the positron traps in the course of annealing of the radiation defects under investigation (E-centers, the divacancies, and, supposedly, the oxygen-related vacancy complexes considered above in sections 4.1–4.3) results only in a certain (comparatively insignificant) decrease of the average positron lifetime: its magnitude remains close to that characteristic of divacancies in the crystal lattice of silicon.

Thus, these findings suggest that the deep donor involves, at least, two vacancies, needless to say that configuration of this center is distorted by a relaxation and that the phosphorus atom, to all appearances, is a component part of this complex.

4. Discussion

Intimately related questions of the positron trapping into shallow and deeper states are discussed below in the light of evidence obtained for the initial material and then for the irradiated one subjected to the detailed isochronal annealing, which, in its turn, resulted in revealing thermally stable point vacancy-type radiation defects demonstrating properties of deep donors.

4.1. Positron annihilation in n-Fz-Si single crystal and related materials: some relevant data

The effects of decrease of the positron lifetime in the temperature interval ∼30–300 K (section 3.1)—unexplainable completely by the thermal compression of the crystal lattice of FZ-Si materials—seem to find a qualitative interpretation on the basis of the assumption that the positron undergoes partial localization at the residual impurity centers whose bonding has ion-covalent character. As the interatomic distance between the as-grown impurity centers is much shorter than the positron diffusion length ($R_N^{(\text{oxygen,carbon})} \ll l_+ = 10^{-5}$ cm [32]), obviously, one can expect effects related to the positron localization at the 'as-grown' oxygen and carbon-related centers which are inevitably present even in the most perfect silicon single crystals. Below we briefly discuss the results obtained in the light of data available on these difficult-to-get-at positron-sensitive centers in silicon.

The experimental data by one way or another related to the shallow states in silicon are rather scarce [6, 7, 24–30].

The oxygen- and carbon-related as-grown defects in silicon may localize positrons so long as the impurity atoms possess much larger electronegativity in comparison with the atoms of silicon: the measured magnitudes are 7.54{8.54} eV, 6.27{7.18} eV, and 4.77{5.32} eV, for the atoms of oxygen, carbon, and silicon, respectively; in the brackets are shown the calculated values obtained by local density approximation, LDA [20]. Being ion-covalent by its own nature, Si–O (or, e.g., Si–C, Si–C–O, etc) bonds bear a negative effective charge [21], thus creating conditions for positron localization (the presence of a free volume in the microstructure of various oxygen- and oxygen–carbon-related as-grown defects in silicon has been widely debated [22, 23]; see also the positron annihilation data on this question [6, 7, 16]).

Also, aggregates such as SiO_n ($n = 2, 4, \ldots$) including oxygen in its electrically inactive forms are a subject of intensive studies in the field of defect engineering in semiconductor technology (see, e.g., [22, 23]).

The phenomenon of the positron localization at both the shallow and deeper states in silicon has been studied by angular correlation of annihilation (ACAR) spectroscopy since the anisotropy of the electron–positron momentum distribution identifying to a certain extent the oxygen-related centers has been observed [24]. In particular, the oxygen-related thermal defects in Cz-Si single crystal were found to trap positrons after heat treatment at 450, 600, and 800–1000 °C [25]. The positions and intensities of both low-intensive central and satellite peaks in ACAR spectra resemble those that have been observed for the as-grown defects in various materials of single crystal quartz [26–28].

It has also been shown that the higher the probability of the positron high-momentum annihilation in the subvalent shells of atoms of the trapping center (P_c), the longer is the average positron lifetime, τ_{av}: in particular, this effect has been observed in passing from some specially selected Cz-Si to the most perfect FZ-Si materials [29]. This regularity suggests the involvement of carbon atoms in the centers which are capable of localizing the positron into the states of large radii both in FZ-Si and Cz-Si materials [30].

The last (but not the least important) aspect of the positron annihilation in silicon is that the elemental specificity of chemically different ion cores of atoms surrounding the positron predetermines the emission of the high-momentum annihilation radiation whose properties affect indirectly the lifetime of positron; to a first approximation, the selectivity of penetration of a positron into the core region of surrounding atoms is controlled both by the efficiency of positron localization and the Coulomb barrier of the ion cores [6, 7, 31].

This fact gives some reasons to infer that the positron states in silicon that are detected by both the positron lifetime measurements [33] are affected by the oxygen-related centers. Their influence on the positron states in silicon was found to determine partial positron annihilation rates both in the interstitial region and subvalent shells [6, 7, 30]. The binding energy of positrons at these shallow traps in silicon is reported to be ∼30 meV [9].

Thus, there are good reasons to believe that the states of that kind affect the temperature dependency of the positron annihilation rate in the initial n-FZ-Si ($[P] \approx 7 \times 10^{15}$ cm^{-3}) material before its irradiation (section 3.1).

Starting from the estimates of the temperature dependency of the lifetime of positrons occupying a shallow trap [9] we attribute a very weak Boltzmann-like temperature distribution of the positron lifetimes to the shallow positron traps in the investigated FZ-Si single crystal (see figure 3). The estimated energy of their ionization (∼0.0133 eV) corresponds to a radius of the hydrogen-like orbit of the charge carrier equal to several tens of interatomic distances.

The long-range Coulomb potential of the negative effective charge of the defect in the silicon lattice is theoretically shown to create weakly bound hydrogen-like Rydberg positron states; the transition rate of the thermalized positrons to the Rydberg states may be rather high [19]. Being shallow and having radius $\sim 10^{-5}$–10^{-6} cm in order of magnitude, these states are characterized by the effective detrapping rate, which, in its turn, complicates their observation by positron annihilation: usually, the detected effects are well marked, but they have comparatively low intensity (a weak temperature dependency of the positron lifetime shown in figure 3 may serve as an illustration of this fact).

Bearing in mind that knowledge about as-grown oxygen-related centers in the technology of silicon is of paramount importance, further, more precise positron probing of these defects is necessary. The results under discussion give good reasons to believe that the positron is trapped into the deeper states related to the radiation defects via these shallow ones; intimate relationships between these two processes of positron localization require further investigations.

4.2. Lifetime of positrons in proton-irradiated n-FZ-Si and configuration of defects

As seen in figure 12, the magnitudes of the positron lifetime calculated by Hakala *et al* [36] for the vacancy and the divacancy are in the region between the values of the

short-lived and the long-lived positron lifetimes reconstructed from the experimental data. The calculation of the positron lifetimes includes the one of the electron density at the positron which was obtained on the basis of the LDA scheme; the effects of exchange and correlation were taken into account and the parametrized enhancement factor of the annihilation rate introduced by Boronski and Nieminen was used (for more details about the schemes of calculation of the lifetime of positrons localized at the vacancy clusters in silicon, see, e.g., [37, 38]).

The short-lived positron lifetime (∼120–140 ps) seems to characterize the excessive partial electron density contacting the trapped positron, as far as some findings available speak in favor of this suggestion. First, the electron effective charge may be redistributed on the nearest neighbors owing to the closing of the dangling bonds of atoms involved into the vacancy-type defects as well as due to the Jahn–Teller distortion of the vacant site [39]. Besides, according to the data of EPR spectroscopy [1] the electron density participating in the hyper-fine interaction is concentrated, mainly, on the paramagnetic quasi-molecule of the phosphorus–vacancy pair. This kind of defect was shown to be traps of positrons [8–10] and the results presented in section 3.11 seem to reflect the annealing of these positron-sensitive defects (i.e. E-centers).

E-centers in the investigated material of n-type seem to create an attractive potential for the positron because the formation of the donor–vacancy pair is accompanied by elimination of two electrons from the conduction band [18, 41].

Indeed, it is argued that up to ∼70% of the electron wave function in the paramagnetic E-center in the material of p-type is distributed on the four atoms neighboring a free volume created by the vacancy [1]. In the material of n-type to be used in the experiments under discussion the negatively charged E-centers, together with the other defects of the radiation origin, are also to contribute to the positron localization. Starting from this, the temperature dependency of the positron trapping coefficient as well as its (roughly) estimated numerical value $\sim(2\text{–}13) \times 10^{17}$ s^{-1} in the temperature interval ∼35–60 K (see figure 9) may characterize the weakly bound positron state of a rather large radius (overlapping a few interatomic distances), which is similar to the one analyzed for a negative ion [4, 19].

It will be observed that ∼70% of the wavefunction of the paramagnetic electron is located on the six atoms surrounding the two vacancies in the molecule of the divacancy [13], which is known to be the positron trap. Effective charges of these localized electrons contribute to the positron trapping coefficient whereas the efficiency of the positron localization at the attractive centers, in its turn, is due to the intensity of the positron–phonon interaction [19, 35]; competition between the trapping and detrapping processes seems to determine the values of the deconvoluted positron lifetimes obtained for at least singly negatively charged divacancies in the investigated material (see, e.g. sections 3.6 and 3.12).

The long-lived positron lifetime ∼270–315 ps is closed to the calculated magnitudes characteristic of the divacancy (∼299 ps, see figure 12); its value, obviously, suggests that the lifetime of the positron is related to vacancy–impurity complexes containing, at least, two vacancies. Presumably, having a concentration $\sim 6 \times 10^{14}$ cm^{-3}, the divacancies are also involved in the formation of the long-lived component (it should be recalled that no larger multi-vacancy defects have been observed in our low-temperature measurements of the electro-physical parameters of the material; see section 2). It should also be mentioned that the experimental data obtained also indicate that E-centers (and to a less extent A-centers, due to their comparatively low concentration in the investigated FZ-Si single crystals) contribute to both the short-lived and long-lived components of the positron lifetimes.

Interestingly, the healing of the radiation defects similar to the one discussed in sections 3.9 and 3.10 has been observed in [16], where the annealing of the radiation defects of a vacancy type produced with 2 MeV electrons ($D_{\text{irr.}} \sim 10^{18}$ cm^{-2}) at $T_{\text{irr.}} = 4$ K in both the low-doped Cz-Si:P and in undoped FZ-Si materials was completed at ∼330–380 °C (in this connection, see, e.g., [16] and figures 1 and 2 therein). The similarity mentioned requires further investigation in the light of the problem of the similarity and distinctions of separation of Frenkel pairs under the proton and electron irradiation of silicon.

4.3. Shallow positron states in the irradiated material

These states are thermally stable, they coexist with the deeper positron states influencing the evolution of the temperature dependences of the positron lifetime over the range of annealing temperature ∼60–340 °C (see figure 21).

These experimental facts indicate that the positron shallow states under discussion are intimately related to the movement and disappearance of divacancies during the annealing.

The activation energy of the stress-induced alignment of divacancies created with 1.5 MeV electrons in FZ-Si crystals of p-type in the course of experiments on EPR was found to be ≈0.06 eV, thus suggesting that the divacancy is capable of propagating in the crystal lattice without dissociation. The estimation made in the work [13] for its binding energy gives the value ≥1.6 eV, and the energy of activation of diffusion of divacancies is ∼1.3 eV. It is also argued that the temperature interval ∼180–260 °C is characteristic of the annealing of divacancies (for more details, see [18] and references therein).

The positron lifetime values to be discussed here for divacancies correlate to a certain extent with the data obtained on the basis of the temperature dependence of a so-called defect-specific parameter that has been determined by the measurements of the Doppler broadening of annihilation radiation for the centers of radiation origin in float-zone-refined silicon having a resistance of 7000 Ω cm [42]. It should be emphasized that the existence of the weakly bound states-precursors appears to be a common feature of the attractive point centers in silicon regardless of whether it concerns the as-grown centers in the crystal or the radiation defects of a vacancy type. The question whether the shallow

positron states are also formed under positron trapping at the E-centers requires a special study.

Implicitly, the smearing of a characteristic hump (wide maximum, see figure 21) resulting from competing positron trapping/detrapping processes (that proceed via shallow states) indicates an efficient role of both the phonon concentration and the energy of phonons in forming the parameters of annihilation in the vicinity of the positron traps. Obviously, the phonon concentration increases quite effectively in the temperature interval ranging from ∼30 to 300 K inasmuch as its value is proportional to $\approx\frac{T}{\theta_D}$ and $\approx\frac{T^3}{\theta_D^3}$ at $T \gg \theta_D$ and $T \ll \theta_D = 645$ K , respectively (θ_D is the Debye temperature). The softening of the phonon spectrum around the centers of a vacancy type is known to contribute to the efficiency of the cascade phonon emission under the process of trapping of the charge carriers [39], thus suggesting the existence of a similar picture for the positron trapping.

In connection with this question here one can mention a typicality of the shallow and deeper positron states to be observed for the point radiation defects of a vacancy type in the positron annihilation studies: e.g., the curve for the temperature dependency of the average positron lifetime measured for the electron-irradiated low-doped Cz-Si:P material ($E_{irr.} = 2$ MeV at 4 K, $D_{irr.} \sim 10^{18}$ cm^{-2}) demonstrates a characteristic maximum (or hump) at somewhat higher temperatures, so that the average positron lifetime begins getting shorter below ∼150 K with decreasing temperature due to the reduced detrapping of positrons from the shallow traps [16].

Interestingly, that appearance of the shallow positron states is not a rare occurrence in studying the positron-sensitive defects in silicon. These states seem to be observed also in the course of annealing of defects in the undoped high-resistance Fz-Si single crystals irradiated with electrons, protons, and ions of high energy [42]; the trapping of positrons via weakly bound (shallow) states in the investigated material was attributed by the authors to the divacancies having neutral charge states.

4.4. Positron trapping under isochronal annealing in the range ∼280–320 °C

As has been described in sections 2 and 3 the positron trapping process has several stages, namely, the early stage of the isochronal annealing proceeds in the temperature interval ∼60–180°C and it includes the disappearance of E-centers, then it follows with the stage having temperature interval ∼180–280°C related to healing the divacancies; the defects to be attributed (tentatively) to A-centers being annealed in the comparatively narrow temperature interval ∼280–320°C (see, e.g., figure 17).

The A-centers are known to be the positron traps contributing to the average positron lifetime [16]. In contrast to Cz-Si material, the concentration of these centers in the proton- and electron-irradiated n-FZ-Si:P material is considerably lower. These defects as well as other vacancy complexes containing oxygen impurity atoms are capable of trapping positrons [42]. The morphology of the oxygen-related positron traps of radiation origin in silicon is unclear and the attribution of the positron annihilation parameters to these defects in silicon requires, as a rule, the use of more complex configurations than that of A-centers, e.g., such as the divacancy–carbon–oxygen complex, V_2–C–O, and others, see, e.g. [6, 7, 25, 41–43] and references therein. However, the A-center may serve as a model of a tentative vacancy–oxygen positron trap inasmuch as it bears a negative effective charge in n-type silicon having the unpaired electron on the deep level. According to the EPR evidence, about 70 percent of the electron density of the unpaired electron is localized on the two nearest neighbors to the oxygen atom, which do not form bonding with it; the remaining electron density is redistributed on the neighboring 12-16 sites of the crystal lattice [14, 15, 18].

On the basis of systematic studies of electron-irradiated n-type silicon it is argued that the lifetime $\tau \approx 225$–230 ps in the temperature interval 20–150 K reflects the positron localized state at the oxygen–vacancy complex in silicon [9] and that a shallow-trap behavior of a localized positron should be attributed to the A-center [16]. In the investigated proton-irradiated material—when the temperature of annealing reaches $T_{anneal.} \approx 300$ °C and the oxygen-related defects of a vacancy type (including A-centers) are assumed to begin dissociating [14–16]—the average positron lifetime changes, ranging from ∼220 ps at $T_{meas.} = 300$ K to ∼252 ps at $T_{meas.} = 30$ K (figure 25), thus suggesting the presence of several channels of annihilation which supposedly also include the ones related to the oxygen-related centers.

4.5. Positron trapping at the beginning of healing of deep donors at $T_{anneal.} \geq 320$ °C

According to the data to be considered in this paper, however, after completing of healing of the radiation defects at the stages under discussion, the investigated material still contains thermally stable point defects possessing properties of deep donors. In this connection, the question whether the annealing of E-centers, the divacancies, and the oxygen-related centers participate in one way or another in forming these deep donor centers—or these point defects are mostly formed in the process of irradiation of the n-FZ-Si material with 15 MeV protons—is still open.

Inasmuch as the average positron lifetime at 30 K decreases, mainly, as the annealing temperature reaches $T_{anneal.} \approx 300$–320 °C, thus, at the beginning of this interval the averaged coefficient of positron trapping (discussed above in sections 3.3, 3.5 and 3.8), to all appearance, should be attributed to the thermally most stable positron traps—that of remaining in the material after the step of the isochronal annealing at $T_{anneal.} \approx 300$ °C (i.e. when E- and A-centers as well as the divacancies have already been annealed). These thermally most stable defects are the deep donors repeatedly considered above; at the temperature of the isochronal annealing $T_{anneal.} \geq 300$ °C they begin to anneal, restoring electrical activity to the phosphorus atoms in the course of annealing (see also section 2.2 where the results of electric measurements are present).

It is interesting that the temperature dependency of the positron trapping coefficient related to the deep donors follows the one calculated for negatively charged vacancies (section 3.7).

The changes of values of the positron trapping coefficient obtained seem to be close to the calculated ones, though the absolute values are different (figure 14); this difference is related to that of the concentration used in the theoretical evaluation of the positron trapping coefficient.

A surprisingly similar behavior of the curves in figure 14 is observable evidence of the multi-phonon-assisted process [40] of the trapping of positrons by the radiation centers under consideration. There are some reasons to believe that these centers were hidden at the earlier stages of the isochronal annealing; however, the behavior of the experimental data obtained for the irradiated material before its annealing is qualitatively similar to that under discussion for the beginning of the last stage of annealing ($T_{\text{anneal.}} \approx$ 300–320 °C: see figure 14); this similarity will be discussed elsewhere.

4.6. Deep donors and electrical activity of phosphorus atoms in proton-irradiated n-FZ-Si material

It has been generally accepted previously that the compensation of shallow donors under the proton irradiation of silicon is due to the formation of deep radiation-induced acceptor states belonging, primarily, to the vacancy complexes of the divacancy type. The results of our study, on the contrary, seem to indicate unambiguously that this is not quite the case for proton irradiation of n-FZ-Si, in which case the rate of carrier removal from the conduction band is mostly determined by the removal rate of shallow donor states (rather than by the formation of the compensating acceptors, see section 2.2 for more detail). It means, in its turn, that the model of compensation of shallow donors by deep acceptor states due to E-centers and divacancies, adopted earlier in the literature (see, e.g. [44]) must be replaced by a more adequate model with a modified reaction path leading to effective 'deactivation' of shallow donors in proton-irradiated n-FZ-Si. It should be recalled that, for the same material irradiated with fast electrons, the model of E-centers formation was shown to be absolutely adequate for describing the observed radiation degradation of electrical parameters [11, 12]. The difference of the defect formation under electron and proton irradiation is thought to be related to the capture of more than one vacancy by a phosphorus atom in the investigated silicon because under the proton irradiation the defects are produced in cascades—in contrast to electron irradiation, where the defects are formed uniformly in the bulk.

The results of this work show that the configuration of the defect playing role in the compensating mechanism of proton-irradiated n-FZ-Si is a defect complex containing a phosphorus atom and two vacancies. The high temperature of annealing indicates that this complex should be a deep donor. However, this defect does not manifest itself in the electrical measurements performed for the n-type material when the Fermi level is shifted from $E_c - 0.21$ eV to $E_c - 0.24$ eV due to proton irradiation (on the contrary, as the data under discussion show, the positron probing of this defect turns out to be quite effective one).

The number of vacancies in the deep donor requires special investigation. In the case where the relaxation of atoms surrounding the volume created by the vacancies is thoroughly taken into account this number may turn out to be equal to three: probable involvement of a trivacancy in the diffusion processes resulting in the formation of complexes with the oxygen impurity in CZ-Si is being rather intensively debated (see [48] and references therein). However, as has already been discussed above in section 2.2, for the moderately doped n-FZ-Si material the formation of compensating acceptors which are characteristic of the vacancy-type defects plays a subordinate role in the process of deactivation of the donor states of the dopant under irradiation with 15 MeV protons [12]. The results obtained in this work give some reasons to believe that in proton-irradiated n-Si (FZ) the electrical activity of the phosphorus atom is very much affected, as is argued in this paper, by formation of a complex including either a divacancy or a couple of vacancies.

The donor level of this vacancy–impurity complex is not detected by the Hall measurements performed in this work, inasmuch as the Fermi level $\sim E_c - 0.21$ eV in the moderately doped n-type FZ-Si material due to a low applied dose of proton irradiation changes its position quite moderately to, approximately, $\sim E_c - 0.24$ eV; this means, nevertheless, that the donor level is at least below this value of energy, i.e. its energy level is at least at $E > E_c - 0.24$ eV, needless to say, it may lie deeper in the forbidden gap.

In this connection one should mention the level $\sim E_c -$ 0.30 eV tentatively attributed to the phosphorus–vacancy pair including a hydrogen atom (s) in proton-irradiated of n-type silicon [49]: the data of these DLTS experiments suggest that this level belongs to the negatively charged deep donor center. Also, earlier the deep donor centers were supposed to be observed in DLTS experiments on 9 MeV electron irradiation of n-type silicon [50].

5. Conclusion

We have studied the positron states and their lifetimes in n-FZ-Si ($[P] \approx 7 \times 10^{15}$ cm^{-3}) single crystal subjected to irradiation with protons having energy $E = 15$ MeV ($T_{\text{irr.}} \approx$ 300 K). The distinguishing feature of this research is that the positron lifetime studies have been carried out in parallel with the analysis of the temperature dependences of the carrier density and mobility measured over the range ~4.2 to 300 K. The samples-satellites to be used for both positron investigations and the electrical measurements were cut from the same wafer. When possible, the experimental evidence is compared with the data of theoretical studies of the defects under investigation.

(1) The movement of positrons in the initial non-irradiated material is characterized by a mixture of the delocalized and localized weakly bound (shallow) states, in which case the positron lifetime slightly decreases with the

temperature ranging from ∼300 to ∼30 K. There are experimentally obtained arguments that residual oxygen-related centers are capable of localizing the positron at the weakly bound states with a roughly estimated energy equal to $E_b \approx 0.013$ eV. The localization of the positron appears to occur due to both availability of negative effective charges in ion-covalent bonding and a small open volume of the as-grown complexes created by the residual impurities in the single crystal of the investigated silicon.

(2) Under doses of irradiation ranging from 4×10^{13} to 8×10^{13} cm^{-2} the defect production in n-FZ-Si $\langle P \rangle$ single crystal with 15 MeV protons at room temperature provides the trapping-limited regime for the trapping of positrons, which, in its turn, determines the average positron lifetime.

(3) Almost 'gigantic' values of the positron trapping coefficient, ranging from $\approx 2 \times 10^{17}$ to $\approx 2 \times 10^{18}$ s^{-1} have roughly been estimated for defects in the material after its irradiation. It was found that the radiation defects include shallow traps of positrons. The occupation of the weakly bound (shallow) states by positrons leads to a decrease of the average positron lifetime when the measurements are conducted at temperatures lower than ∼66–100 K. At higher temperatures the shallow positron states (probably, the Rydberg-like ones) are ionized.

(4) On the whole, for the radiation defects produced, over the temperature range ∼100–300 K the positron trapping and detrapping processes are controlled by the centers in which the positrons are bound in the states with energy ∼0.04–0.07 eV.

(5) The parameters of the partial components of the average positron lifetime reconstructed in the course of the many-stage isochronal annealing follow the changes of both the microstructure and concentration of defects to be detected by the temperature dependences of the carrier density and mobility measured over the range ∼4.2–300 K. The positron traps whose microstructure is changed in the course of the isochronal annealing within the ∼180–260 °C temperature range are identified as divacancies; this stage follows the stage of annealing of E-centers (∼60–180 °C) which are the positron traps, too. The annealing of the positron traps in the interval ∼260–300 °C is tentatively attributed to the oxygen-related centers.

(6) After the disappearance of E-centers and divacancies, the shallow positron states ($E_b \leq 0.01$ eV) are still observed up to temperatures of ∼320–340 °C in the course of isochronal annealing of the proton-irradiated n-type FZ-Si material under investigation. Together with these weakly bound states, the positron trapping by the point defects of a vacancy type having properties of deep donors has been observed at this stage of annealing.

(7) The most effective recovery of the average positron lifetime begins at $T_{\text{anneal.}} \geq 300$ °C and continues up to a value which is characteristic of initial non-irradiated material. The beginning of this stage coincides with the maximal concentration of the deep donors of radiation origin. These defects were hidden from observation at the earlier stages of annealing. They have reliably been observed by positron lifetime spectroscopy in the course of annealing up to $T_{\text{anneal.}} \approx 500$ °C. Meanwhile, the healing of these defects, according to the data of electrical measurements, continues up to $T_{\text{anneal.}} \approx 650$ °C.

(8) The binding energy of positrons at the deep donors is $E_b \approx 0.096 \pm 0.013$ eV for the temperature interval ∼200–270 K, and it changes to a lower value of $E_b \approx 0.021 \pm 0.001$ eV for the range of lower temperatures ∼166–66 K. The positron trapping coefficient increases from $\sim 1.1 \times 10^{16}$ to $\sim 6.5 \times 10^{17}$ s^{-1} over the temperature range ∼266–66 K. This increase is described by a $\approx T^{-3}$ law, thus indicating a phonon-assisted cascade mechanism of the positron trapping by the deep donors.

(9) Both the activation energy of annealing $E_a \approx 0.74$–0.59 eV and the first order of reaction describe the dissociation of the deep donors in the course of isochronal annealing over the temperature range ∼300–650 °C. The annealing of the deep donors is accompanied by the restoration of electrical activity of the phosphorus atoms.

(10) The bulk of evidence suggests that the deep donor of the radiation origin is a complex including one atom of phosphorus and at least two vacancies. Its energy level is at least at $E > E_c - 0.24$ eV in the investigated material.

Acknowledgments

We are indebted to the German Academic Exchange Service (DAAD) and the Condensed Matter and Statistical Physics Section (CMSP) at the Abdus Salam International Center for Theoretical Physics (ICTP) for financial assistance. NA is especially grateful to Professor V E Kravtsov (CMSP at ICTP) for fruitful discussions.

References

[1] Watkins G D and Corbett J W 1964 *Phys. Rev.* **134** A1359
[2] Nylandsted Larsen A and Mesli A 2007 *Physica* B **401/402** 85
[3] Kozlovski V V, Kozlov V A and Lomasov V N 2000 *Semiconductors* **34** 123
[4] Puska M J, Corbel C and Nieminen R N 1990 *Phys. Rev.* B **41** 9980
[5] Hodges C H 1974 *J. Phys. F: Met. Phys.* **4** L230
[6] Arutyunov N Y and Emtsev V V 2005 *Solid State Phenom.* **108/109** 615
[7] Arutyunov N Y and Krause-Rehberg R 2004 *Solid State Phenom.* **95/96** 507
[8] Makinen J, Hautojarvi P and Corbel C 1992 *J. Phys.: Condens. Matter* **4** 5137
[9] Krause-Rehberg R and Leipner H S 1999 *Positron Annihilation in Semiconductors* (Berlin: Springer)
[10] Makinen J, Corbel C, Hautojarvi P, Moser P and Pierre F 1989 *Phys. Rev.* B **39** 10162
[11] Kozlovski V V, Emtsev V V, Emtsev K V, Strokan N B, Ivanov A M, Lomasov V N, Oganesyan G A and Lebedev A A 2008 *Semiconductors* **42** 243

[12] Kozlovski V V, Emtsev V V, Ivanov A M, Lebedev A A, Oganesyan G A, Poloskin D S and Strokan N B 2009 *Physica* B **404** 4752
[13] Watkins G D and Corbett J W 1965 *Phys. Rev.* **138** A543
[14] Watkins G D and Corbett J W 1961 *Phys. Rev.* **121** 1001
[15] Corbett J W, Watkins G D, Chrenko R M and McDonald R S 1961 *Phys. Rev.* **121** 1015
[16] Polity A, Börner F, Huth S, Eichler S and Krause-Rehberg R 1998 *Phys. Rev.* B **58** 10363
[17] Kozlovski V V, Emtsev V V, Ivanov A M, Kozlovski V V, Lebedev A A, Oganesyan G A and Strokan N B 2010 *Semiconductors* **44** 678
[18] Emtsev V V and Mashovets T V 1981 *Impurities and Point Defects in Semiconductors* (Moscow: Radio i Svyaz')
[19] Puska M J and Nieminen R N 1994 *Rev. Mod. Phys.* **66** 841
[20] De Proft F and Geerlings P 1997 *J. Chem. Phys.* **106** 3270
[21] Claeys C and Vanhellemont J 1989 *Solid State Phenom.* **6/7** 21
[22] Endrös A L 1993 *Solid State Phenom.* **32/33** 143
[23] McCluskey M D, Hsu L and Lindstrom J L 2003 *Physica* B **340–342** 514
[24] Arutyunov N Y and Trashchakov V Y 1989 *Solid State Phenom.* **6/7** 435
[25] Arutyunov N Y, Emtsev V V, Schmalz K and Trashchakov V Y 1990 *Phys. Status Solidi* a **121** K163
[26] Arutyunov N Y, Sobolev N A, Trashchakov V Y and Chek E I 1990 *Sov. Phys. Semicond.* **24** 1112
[27] Arutyunov N Y 1993 *Solid State Phenom.* **32/33** 589
[28] Arutyunov N Y 1997 *Solid State Phenom.* **57/58** 489
[29] Arutyunov N Y 1999 *Solid State Phenom.* **69/70** 333
[30] Arutyunov N Y and Trashchakov V Y 2002 *Solid State Phenom.* **82–84** 795
[31] Arutyunov N Y 2007 *Condensed Matter: New Research* ed M P Das (New York: Nova Science Publishers) p 297
[32] Makinen S 1992 *Mater. Sci. Forum* **105–110** 369
[33] Gebauer J, Rudolf F, Polity A, Krause-Rehberg R, Martin J and Becker P 1999 *Appl. Phys.* A **68** 411
[34] Brandt W 1974 *Appl. Phys.* **5** 1
[35] Manninen M and Nieminen R M 1981 *Appl. Phys.* A **26** 93
[36] Hakala M, Puska M J and Nieminen R M 1998 *Phys. Rev.* B **57** 7621
[37] Barbiellini B, Puska M J, Korhonen T, Harju A, Torsti T and Nieminen R M 1996 *Phys. Rev.* B **53** 16201
[38] Saito M and Oshyiyama A 1996 *Phys. Rev.* B **53** 7810
[39] Stoneham A M 1975 *Electronic Structure of Defects in Insulators and Semiconductors* (Oxford: Clarendon)
[40] Abakumov V N, Perel V I and Yassievich I N 1978 *Sov.—Phys. Semicond.* **12** 1
[41] Carter J R Jr 1970 *Phys. Chem. Solids* **31** 2405
[42] Dannefaer S, Avalos V, Kerr D, Poirier R, Shmarovoz V and Zhang S H 2006 *Phys. Rev.* B **73** 115202
[43] Lindström J L, Murin L I, Hallberg T, Markevich V P, Svensson B G, Kleverman M and Hermansson J 2002 *Nucl. Instrum. Methods Phys. Res.* B **186** 121
[44] Kauppinen H, Corbel C, Skog K, Saarinen K, Laine T, Hautojarvi P, Desgardin P and Ntsoenzok E 1997 *Phys. Rev.* B **55** 9598
[45] Damask A C and Dienes G J 1963 *Point Defects in Metals* (New York: Gordon and Breach)
[46] Elsayed M, Krause-Rehberg R, Anwand W, Butterling M and Korff B 2011 *Phys. Rev.* B **84** 195208
[47] West R N 1973 *Adv. Phys.* **22** 263
[48] Markevich V P, Peaker A R, Hamilton B, Lastovskii S B, Murin L I, Cautinho J, Markevich A V, Rayson M J, Briddon P R and Svensson B G 2012 *Physica* B **407** 2974
[49] Palmetshofer L and Reisinger J 1992 *J. Appl. Phys.* **72** 2145
[50] Wada T, Yasuda K, Ikuta S, Takeda M and Masuda H 1977 *J. Appl. Phys.* **48** 2145